Fundamentals of Fan Aeroacoustics

Overview of Lecture

- **Noise Sources and Generation Mechanisms**
  - **Sources of Noise for Typical Fans**
  - **Fluid-Structure Interaction as a Noise Generation Mechanism**
  - **Coupling to the Duct: Propagating Modes and Cut-off Phenomena**
- **Modeling of Fan Noise**
  The Acoustic Analogy
  Computational Methods:Aeroacoustics and UnsteadyAerodynamics
  The Linear Cascade Model
  Effects of Geometry and Blade Loading on Acoustic Radiation
- **Recent Developments in Fan Modeling**
  - **Tonal and Broadband Noise**
  - **Nonuniform Mean Flow Effects:swirl**
  - **Three-Dimensional Effects**
  - **High Frequency Effects**
- **Conclusions**

Dominant Noise Sources for Turbofan Engines

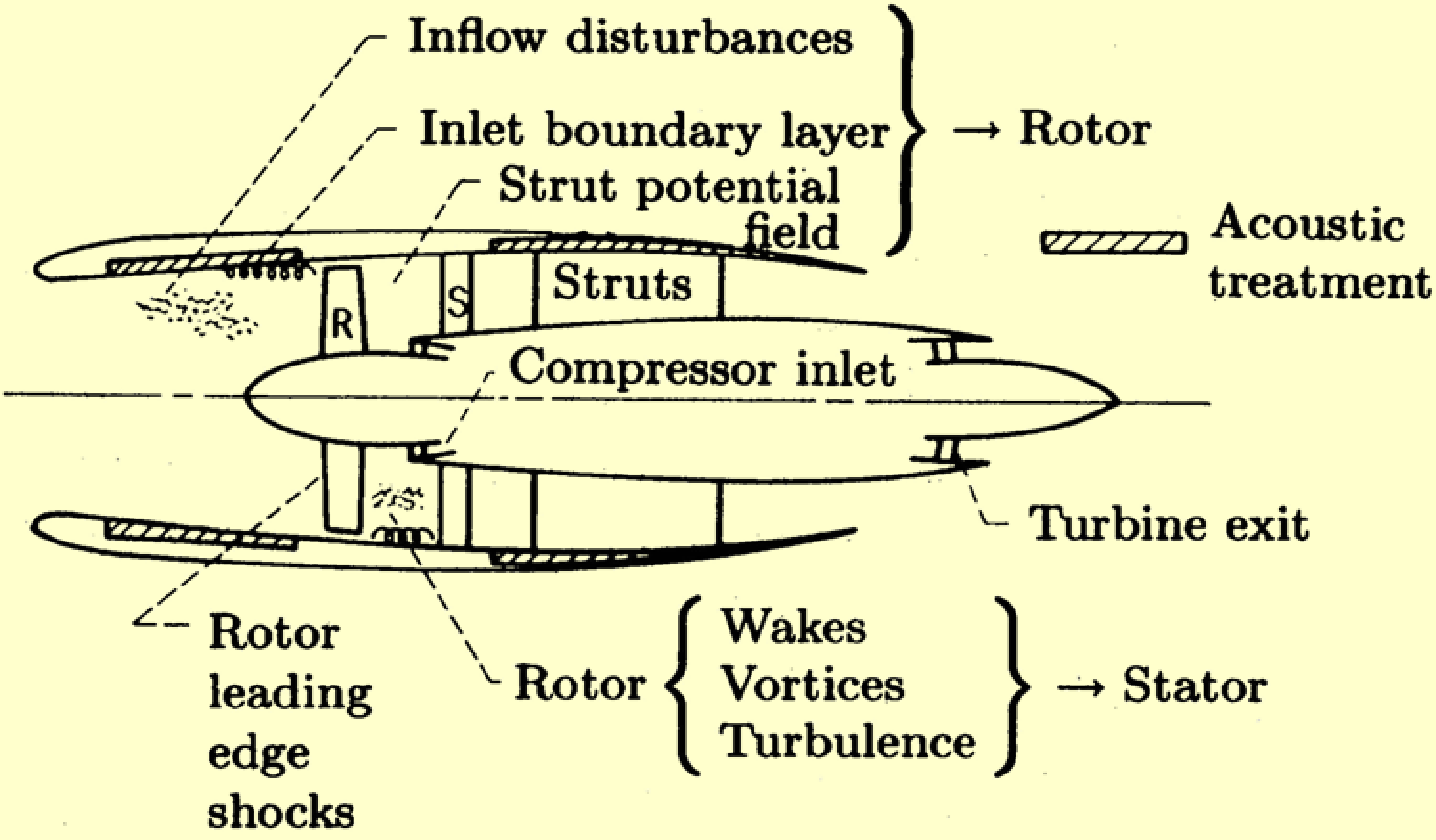

High Bypass Ratio Fan Flyover Noise Maximum Perceived Noise Level

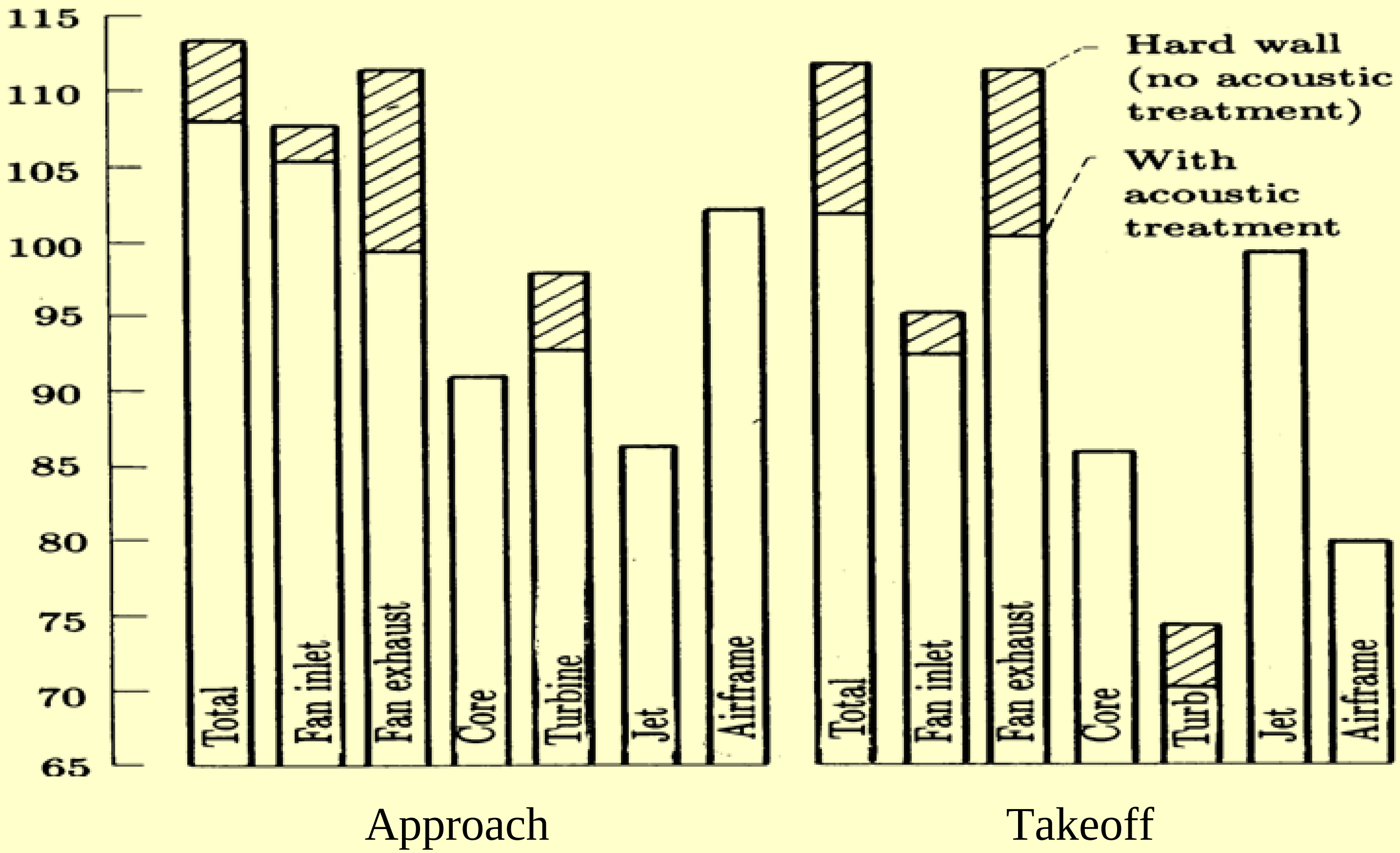

Typical Turbomachinery Sound Power Spectra

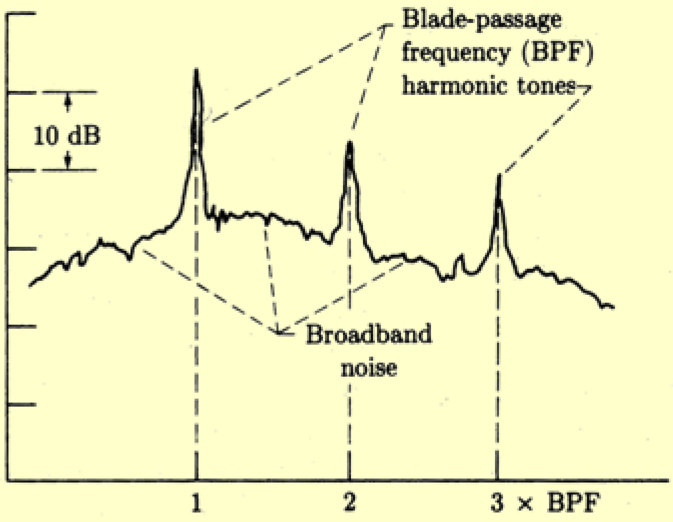

Subsonic Tip Speed

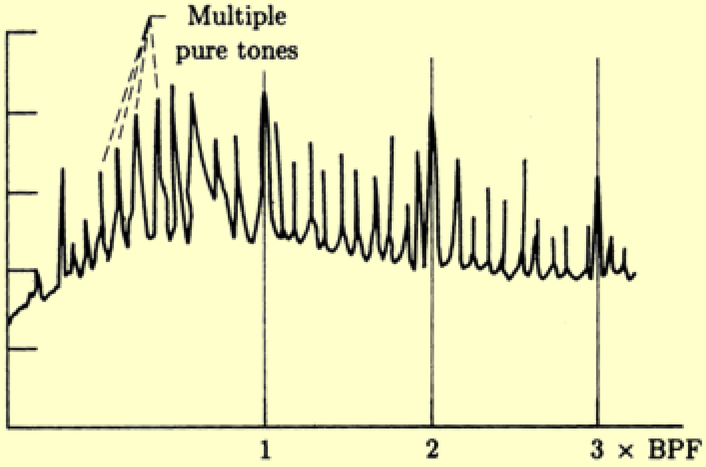

Supersonic Tip Speed

Turbomachinery Noise Generation Process

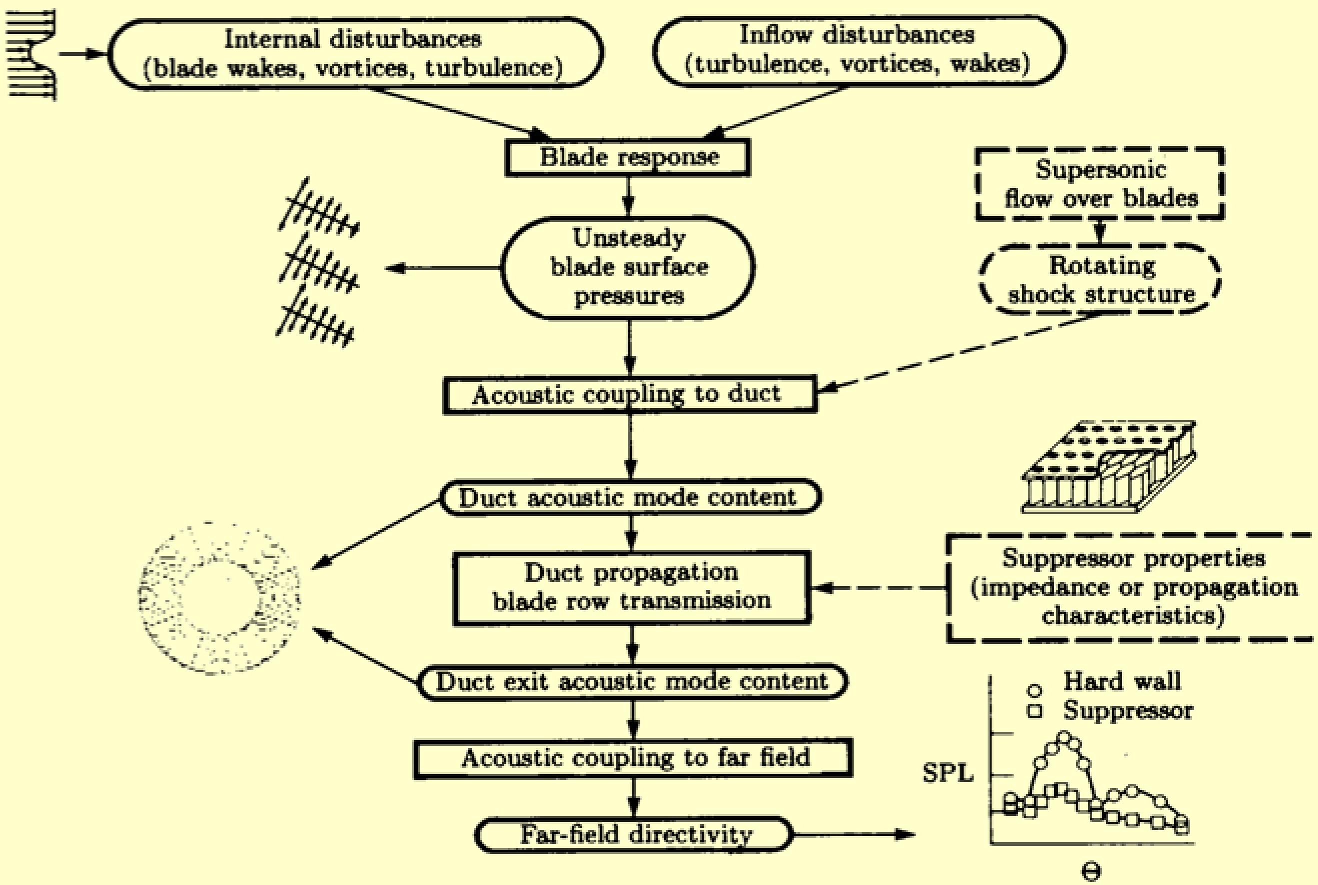

Rotor-Stator Interaction

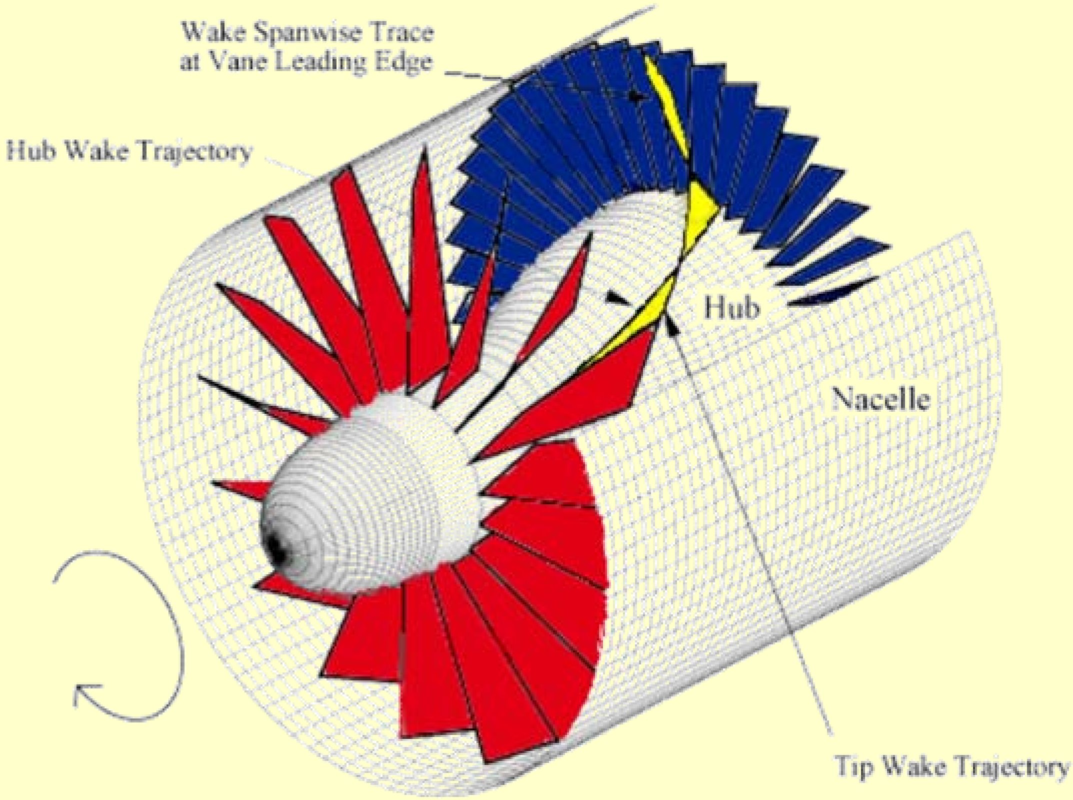

Fluid-Structure Interaction as a Noise Generation Mechanism

- The interaction of nonuniform flows with structural components such as blades and guide vanes produce fluctuating aerodynamic forces on the blades and radiates sound in the farfield.

- Noise Sources: Flow Nonuniformities: Inlet Turbulence, Boundary Layers, Tip and Hub Vortices,Wakes etc.

- Mechanism: Interaction with Rotating Components (rotor noise), Scattering by Sharp Edges (trailing edge noise), Impingement of Unsteady Nonuniformities on Guide Vanes (rotor/stator interaction).

- Propagation in the Duct: Sound Must Propagate in a Duct: therefore only high frequency acoustic modes will propagate.

Rotor Wake Phenomena

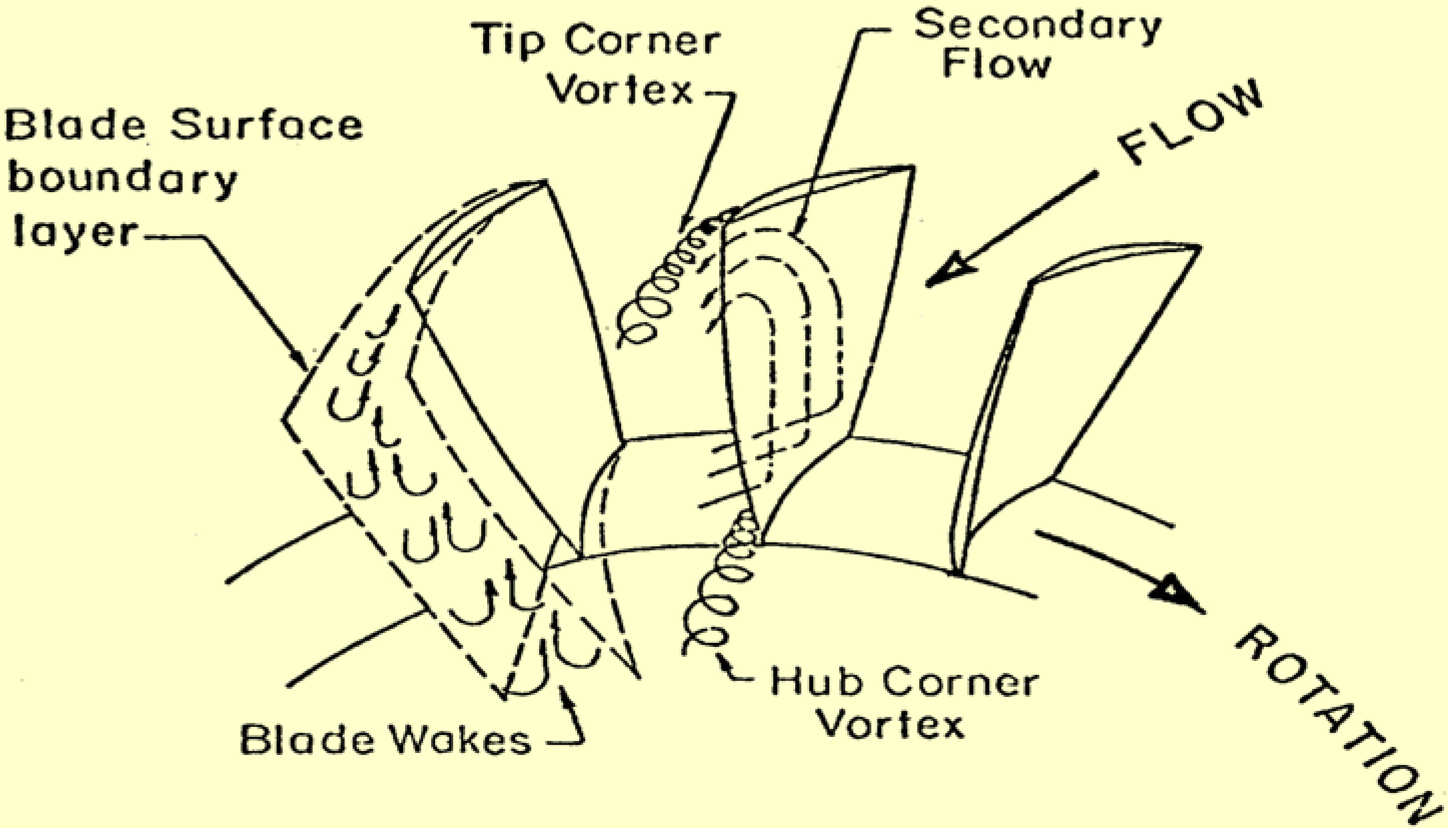

Rotor Wakes Interaction with Downstream Stator

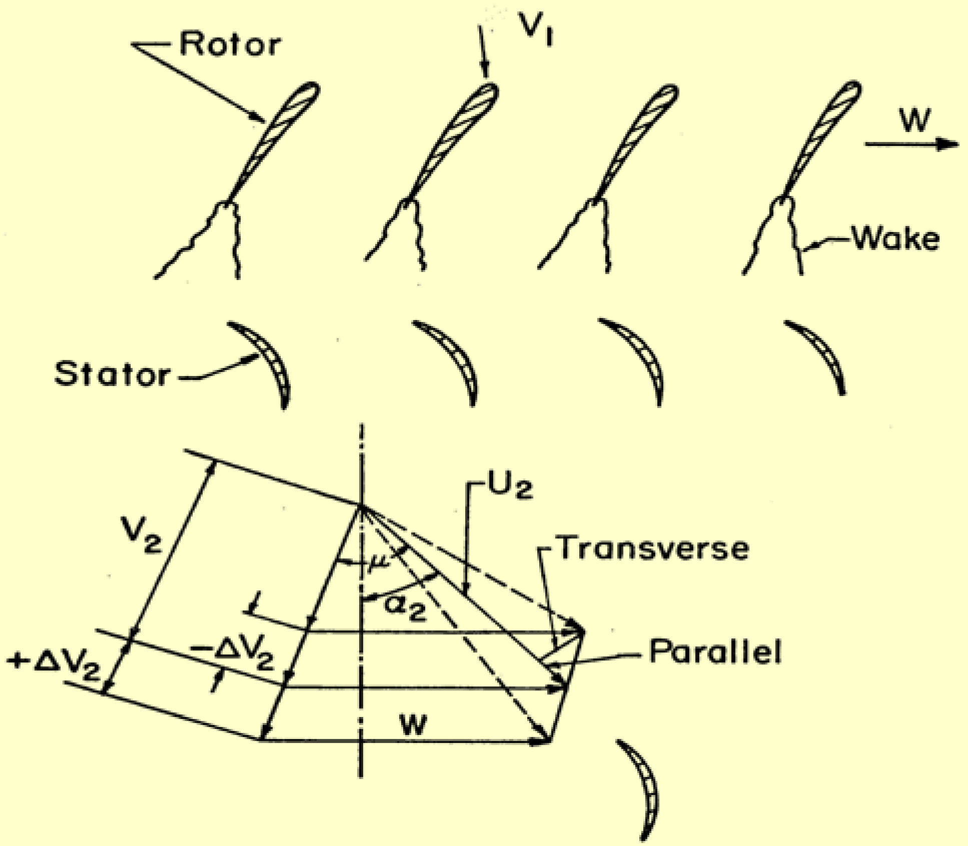

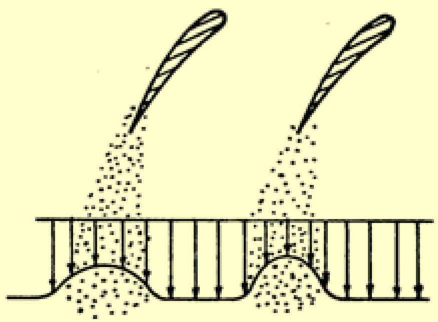

Wakes
Source of unsteady flow

Rotor-Stator Interaction
Wakes and Tip Vortices

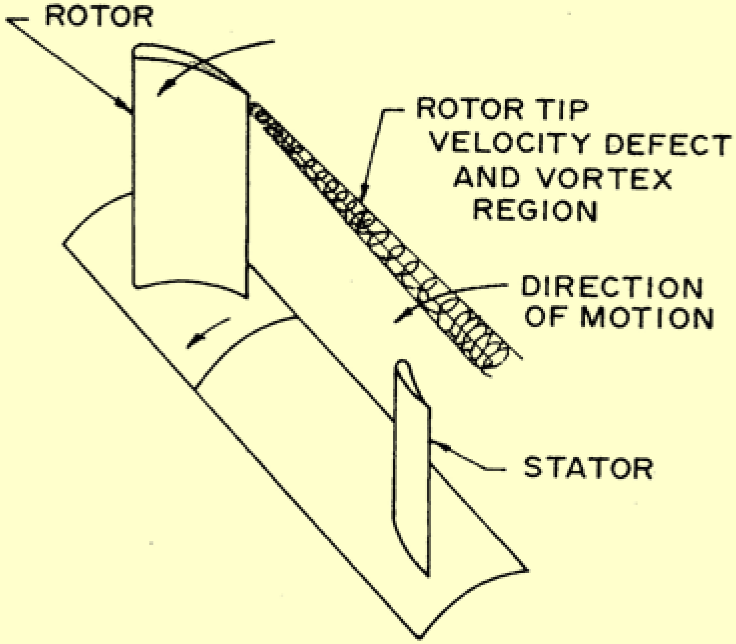

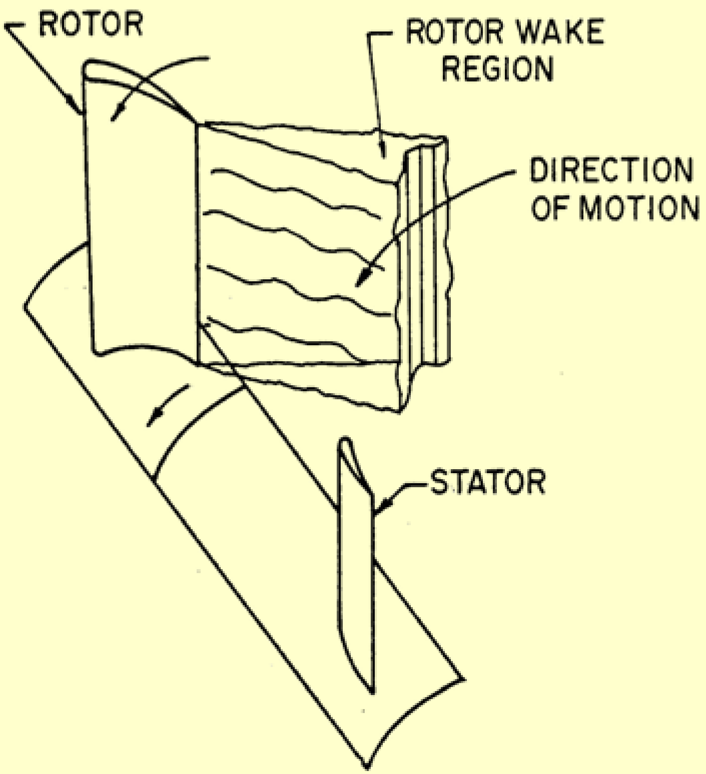

Scaling Analysis

- Multiple length scales:
  - Duct hub and tip Radii: R_h, R_t, Rotor/stator spacing: L
  - Chord length c, Blade spacing s=2pR/(B or V)
  - Turbulence Integral Scale = Λ << c <<R
- Multiple Frequency Parameters:

$$\frac{\omega R}{c_o} = \frac{B \Omega R}{c_o} = BM_\theta >> 1 \qquad \frac{\omega \Lambda}{U_x} = \left(\frac{B \Lambda}{R}\right)\left(\frac{U_s}{U_x}\right) = O(1)$$

- Fast Variables: $\vec{\tilde{x}} = \dfrac{\vec{x}}{\Lambda}$
- Slow Variables: $\vec{x}^* = \dfrac{\vec{x}}{R}$

Blade passing frequency BPF=BΩ

Multiple Pure Tones

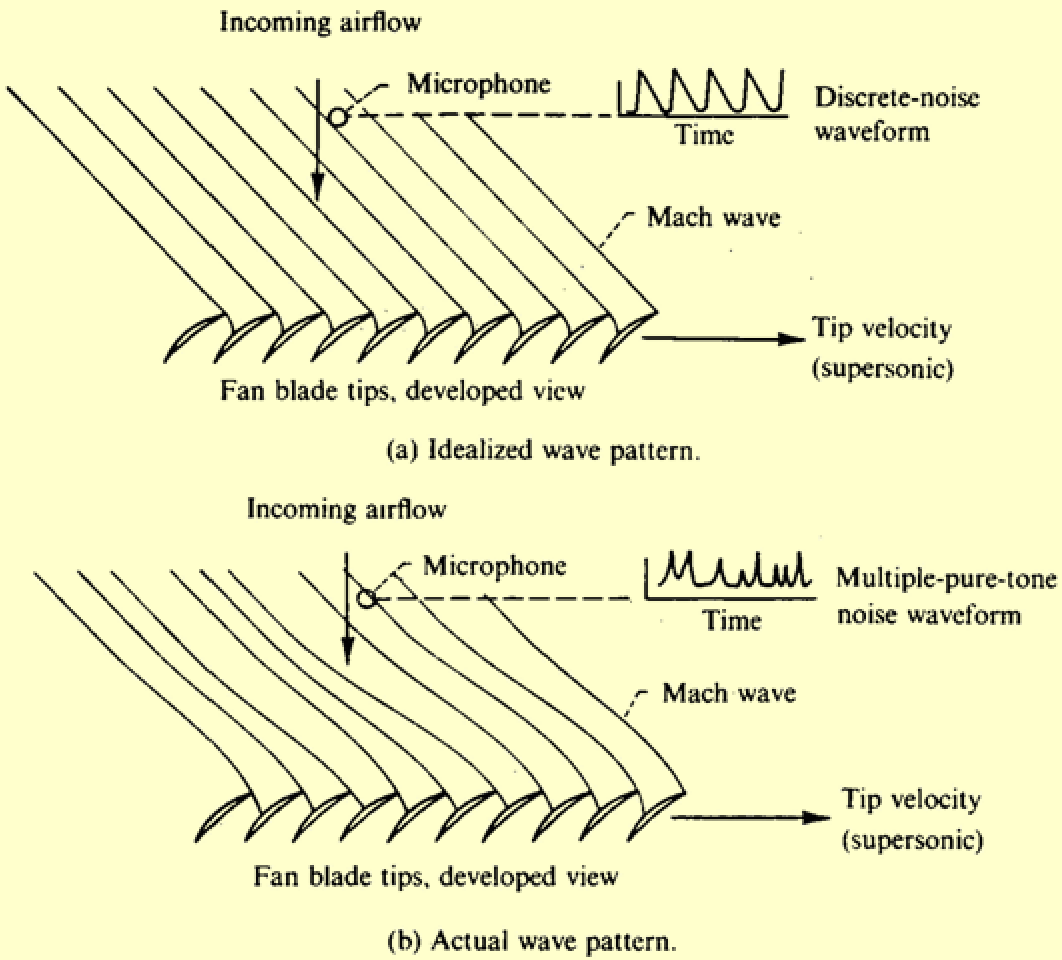

(b) Actual wave pattern.

Airfoil in Nonuniform Flow

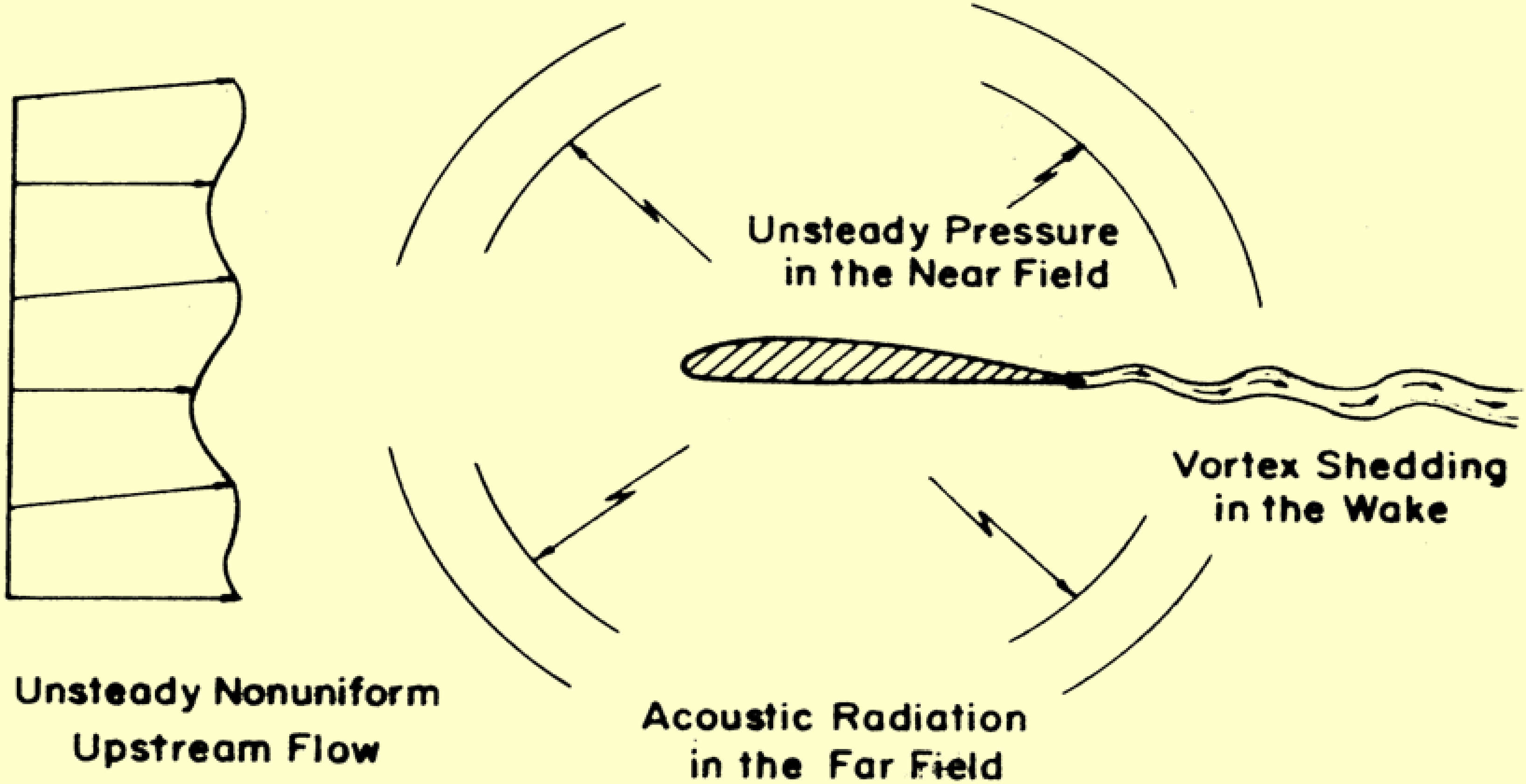

Equations of Classical Acoustics

$$p = p_0 + p'$$

$$\rho = \rho_0 + \rho'$$

$$|\vec{u}| << c_0$$

$$\frac{\partial \rho'}{\partial t} + \rho_0 \nabla \cdot \vec{u} = 0$$

$$\frac{\partial \vec{u}}{\partial t} + \frac{1}{\rho_0} \nabla p' = 0$$

$$(\nabla^2 - \frac{1}{c_0^2} \frac{\partial^2}{\partial t^2}) p' = 0$$

Acoustic Intensity and Energy

- Fundamental Conservation Equation

$$\frac{\partial E}{\partial t} + \nabla \cdot \vec{I} = 0$$

$$E = \frac{p'\rho'}{2\rho_0} + \frac{\rho_0 u^2}{2}$$

$$\vec{I} = p'\vec{u}$$

Fundamental Solution of the wave Equation

- Spherical symmetry:

$$\Phi = \frac{f\left(t \mp \frac{R}{c}\right)}{R}, \quad R = |\vec{x} - \vec{y}|$$

- Green's Function

$$G(\vec{x}, t \mid \vec{y}, \tau) = \frac{\delta\left(t - \tau - \frac{R}{c}\right)}{R}$$

t-R/c: retarded time

- Compact/Noncompact Sources

Causality determines the sign: Sound must propagate away from the source

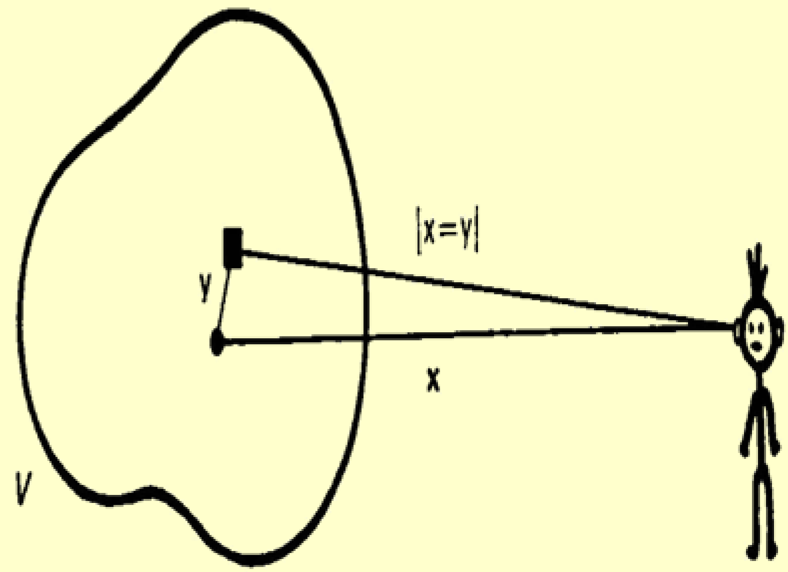

Plane Waves

$$p' = \bar{p} e^{i(\vec{k}\cdot\vec{x}-\omega t)}$$

$$\vec{u} = \frac{\bar{p}}{\rho_0 c_0}\frac{\vec{k}}{k} e^{i(\vec{k}\cdot\vec{x}-\omega t)} = \frac{p'}{\rho_0 c}\frac{\vec{k}}{k}$$

$$E = \frac{p'\rho'}{2\rho_0} + \frac{\rho_0 u^2}{2} = \frac{p'^2}{\rho_0 c_0}$$

$$\vec{I} = p'\vec{u} = \frac{p'^2}{\rho_0 c_0}\frac{\vec{k}}{k}$$

$$\bar{I} = \frac{1}{2}\frac{\bar{p}^2}{\rho_0 c_0}$$

Elementary Solutions of the Wave Equation
No Flow

Noise Source	Acoustic Pressure	Acoustic Intensity	Directivity
Point Source	$\dfrac{\ddot{m}(t - R/c)}{4\pi R}$	$\dfrac{\ddot{m}^2 (t - \frac{R}{c})}{16\pi^2 \rho_0 R^2 c}$	Sperical symmetry
Dipole: Force	$\dfrac{\dot{\vec{\mathrm{F}}}(\mathrm{t} - \mathrm{R}/\mathrm{c}).\vec{\mathrm{e}}_{\mathrm{r}}}{4\pi \mathrm{Rc}}$	$\dfrac{x_i x_j}{16\pi^2 \rho c^3 R^4} \dfrac{dF_i}{dt} \dfrac{dF_j}{dt}$	$\cos\theta$
Quadrupole: Stress	$\dfrac{\ddot{T}_{ij} V x_i x_j}{4\pi R^3 c^2}$	$\dfrac{\ddot{T}_{ij} \ddot{T}_{kl} V^2 x_i x_j x_k x_l}{16\pi^2 \rho R^6 c^4}$	$\cos\theta \sin\theta$

Directivity of Elementary Sources of sound

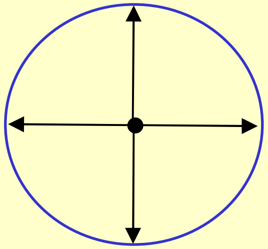

Monopole Directivity

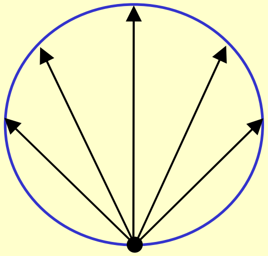

Dipole Directivity

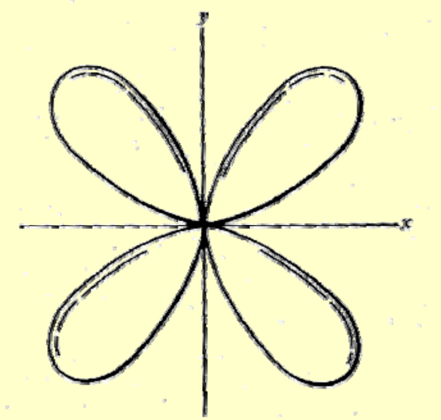

Quadrupole Directivity

Scaling of of Acoustic Power Radiated for Aerodynamic Applications at Low Mach Number

Source	Scaling	Ratio
Dipole	M^6	1
Quadrupole	M^8	M^2

Thus at low Mach number dipoles or forces are more efficient sources of noise than quadrupoles or turbulence. However, this result is valid only for uniform flows and low frequency.

Vortex in a Strongly Nonuniform Flow at Low Mach Number

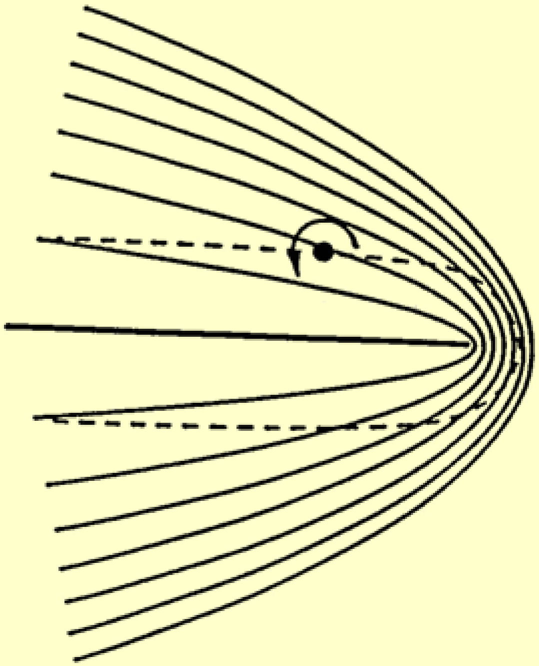

As the vortex travels near the trailing edge it is no longer convected by the mean flow. Its trajectory crosses the undisturbed mean flow. This increases the amount of fluid energy converted into acoustic energy. The acoustic power scales with M^3, much higher than that predicted by a dipole (M^6).

Acoustic Waves in Ducts
Square Duct

- Higher order modes

$$p' = \cos\frac{m\pi x_2}{a}\cos\frac{m\pi x_3}{a}\left[A_{mn}e^{i(k_{mn}x_1-\omega t)} + B_{mn}e^{-i(k_{mn}x_1+\omega t)}\right]$$

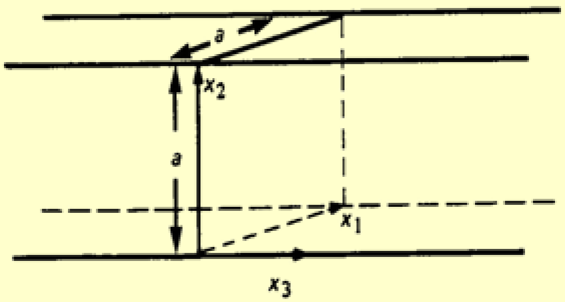

- Dispersion Relation

$$k_{mn} = \sqrt{\frac{\omega^2}{c^2} - \frac{\pi^2}{a^2}(m^2 + n^2)}$$

- Propagating or Cut-on Modes
  - k_{mn}:real

  Evanescent Modes
  - k_{mn}: imaginary

Plane waves always propagate. Higher order modes propagate only when

$$\omega > \frac{\pi c}{a} \text{ or } \lambda < 2a$$

The velocity and pressure of evanescent or cut-off modes are out of phase and there is no net transport of energy (I=0).

Phase and Group Velocities for Dispersive Waves

- Phase Velocity

$$c_{ph} = \frac{\omega}{k} = \frac{c}{\sqrt{1 - \pi^2 (m^2 + n^2) \frac{c^2}{a^2 \omega^2}}}$$

  - Phase velocity is larger than the speed of sound

- Group Velocity

$$c_g = \frac{d\omega}{dk} = c\sqrt{1 - \pi^2 (m^2 + n^2) \frac{c^2}{a^2 \omega^2}}$$

  - Group velocity is the velocity at which acoustic energy is transported in the duct. It is smaller than the speed of sound.

Higher Acoustic Modes in a Duct

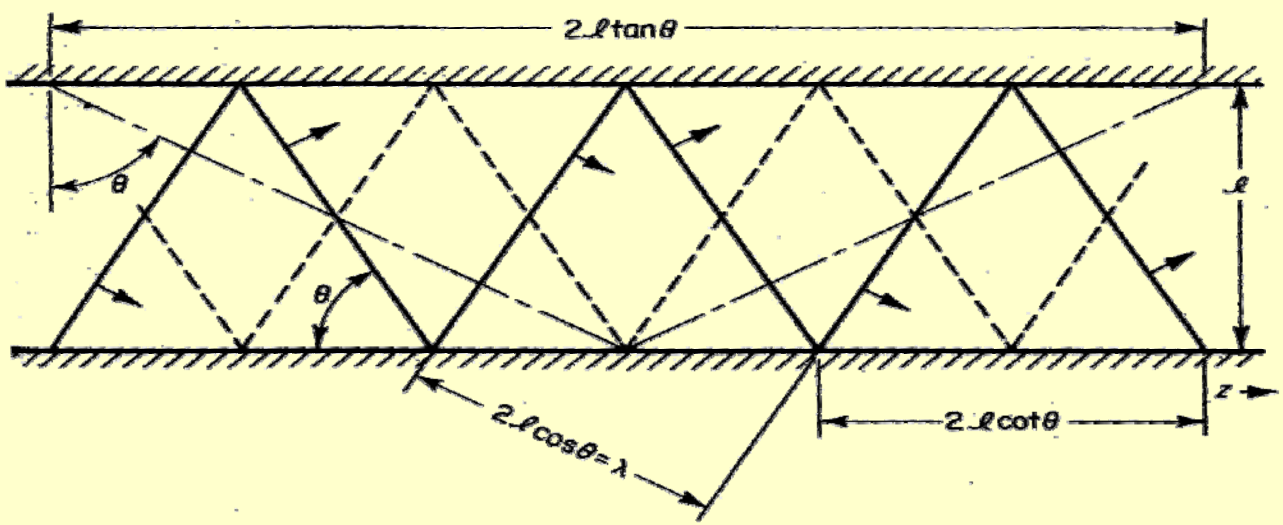

- Reflecting wave components making up the first higher mode propagating between two parallel plates. Solid lines represent pressure maxima of the wave; dotted lines, pressure minima. Arrows, representing direction of propagation of the components, are normal to the wavefronts.

Application to Rotor/Stator Interaction
The Tylor-Sofrin Modes

- Incident Gust $\vec{u}_g = \vec{a}_m^{(g)}(r)e^{i(k_g x + m'\theta - \omega t)}, \quad k_g = \frac{\omega}{U}$
  - Interblade phase angle

$$\sigma = m'\vartheta = m'\frac{2\pi}{V}$$

- Cut-on Modes

$$\vec{u}_a = \sum_{m,n} \vec{a}_{m,n}(r)e^{i(k_{mn}x + m\theta - \omega t)}$$

$$m = m' - qV$$

- For rotor/stator interaction with B rotor blades and V guide vanes

$$m' = pB,$$

- Hence
  - The circumferential modal number m for propagating modes for a rotor with B blades and a stator with V blades is given by

$$m = pB - kV$$

Example: B=18, V=40. m=-22, -4, 10, 14, 22

Sound Propagation in a Duct with Uniform Flow

- The governing equation

$$\frac{D_0^2 p'}{D t^2} + \nabla^2 p' = 0$$

- With the boundary condition at the hub and the tip

$$\frac{\partial p'}{\partial r} = 0$$

- The eigenvalues are given by,

$$k_{mn} = \frac{-\tilde{\omega} M_x \pm \sqrt{\tilde{\omega}^2 - (1 - M_x^2)(m^2 + \gamma_{mn}^2)}}{(1 - M_x^2)}$$

Where

$$\tilde{\omega} = \omega - m M_s$$

- The solution is given by

$$p' = \sum_{m=-\infty}^{\infty} \sum_{n=0}^{\infty} K_n(\gamma_{mn} r) e^{i(k_{mn} x + m\theta - \omega t)}$$

Conclusions

- Fan noise sources: Flow nonuniformities and irregular flow pattern.
- Mechanism: Fluid/structure interaction and link to unsteady aerodynamics.
- Classical acoustics concepts are essential to understanding and modeling of noise.
- The coupling to the duct determines the modal content of the scattered sound and affects sound propagation.

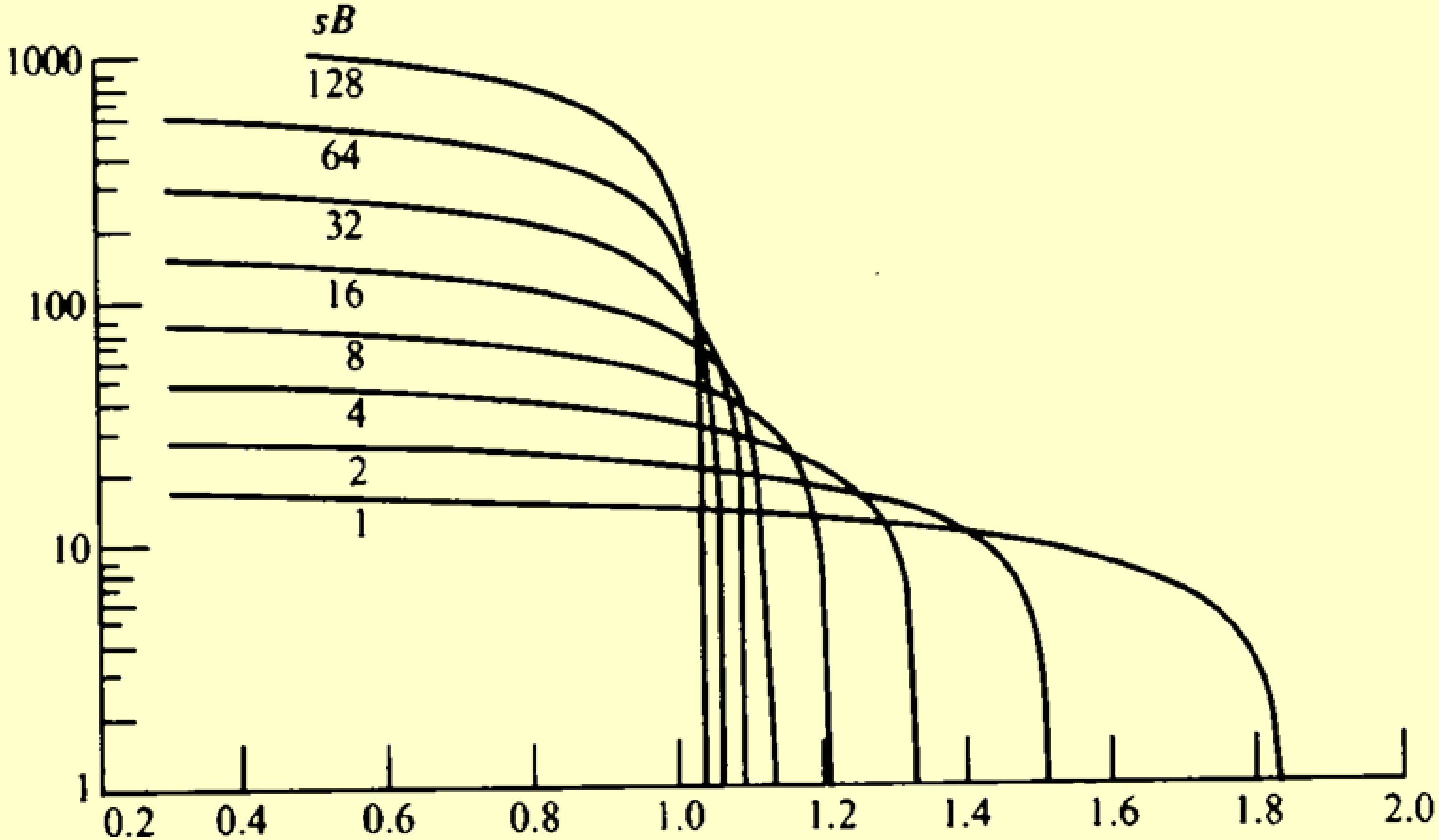
sB
128
64
32
16
8
4
2
1
1000
100
10
1
0.2
0.4
0.6
0.8
1.0
1.2
1.4
1.6
1.8
2.0

Modeling of Fan Noise

- **The Acoustic Analogy**
- **Computational Methods: Aeroacoustics and Unsteady Aerodynamics**
- **The Linear Cascade Model**
- **Effects of Geometry and Blade Loading on Acoustic Radiation**

Lighthill's Acoustic Analogy

- Inhomogeneous wave equation

$$\frac{\partial^2 \rho}{\partial t^2} - c_0^2 \nabla^2 \rho = \frac{\partial^2 T_{ij}}{\partial x_i \partial x_j}$$

- Lighthill's stress tensor

$$T_{ij} = \rho v_i v_j + \delta_{ij}(p - c_0^2 \rho) - e_{ij}$$

$$e_{ij} = \mu\left(\frac{\partial v_i}{\partial x_j} + \frac{\partial v_j}{\partial x_i}\right) - \frac{2}{3}\mu\delta_{ij}\frac{\partial v_k}{\partial x_k}$$

- For a Uniform Mean Flow

$$\frac{D_0^2 \rho}{\partial t^2} - c_0^2 \nabla^2 \rho = \frac{\partial^2 T_{ij}}{\partial x_i \partial x_j}$$

Aeroacoustics and Unsteady Aerodynamics

- Sound is the far-field signature of the unsteady flow.
- Unsteady aerodynamics has been developed for aeroelastic problems such as flutter and forced vibrations where the main interest is to determine the near-field body surface forces.
- The aeroacoustic problem is similar to that of forced vibration but with emphasis on the far-field. It is a much more difficult computational problem whose outcome depends on preserving the far-field wave form with minimum dispersion and dissipation.
- Inflow/outflow nonreflecting boundary conditions must be derived to complete the mathematical formulation as a substitute for physical causality.

Airfoil in Nonuniform Flow

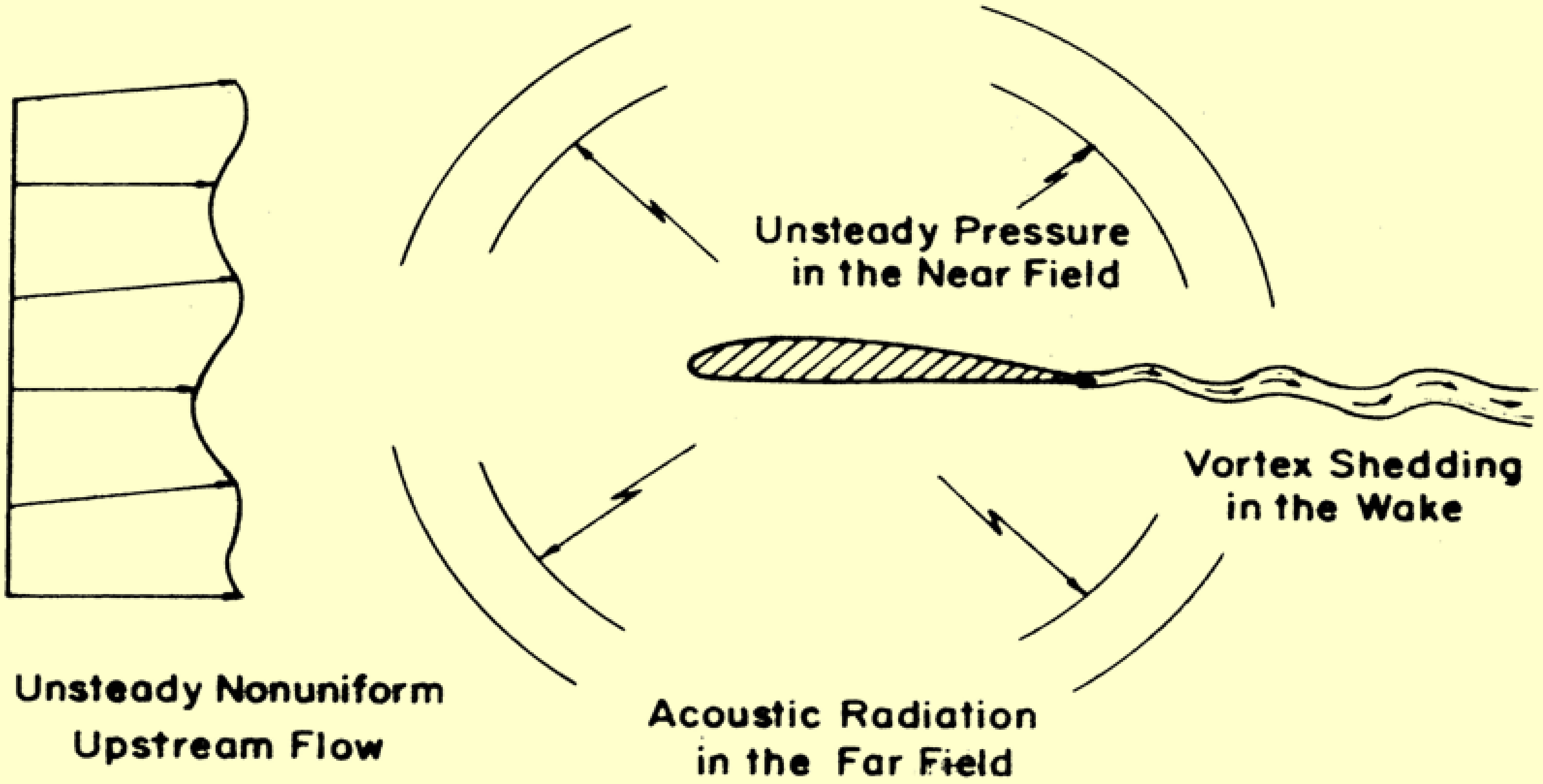

Disturbaces in Uniform Flows

Splitting Theorem:

The flow disturbances can be split into distinct potential(acoustic), vortical and entropic modes obeying three independent equation.

- The vortical velocity is solenoidal, purely convected and completely decoupled from the pressure fluctuations.
- The potential (acoustic) velocity is directly related to the pressure fluctuations.
- The entropy is purely convected and only affects the density through the equation of state.
- Coupling between the vortical and potential velocity occurs only along the body surface.
- Upstream conditions can be specified independently for various disturbances.

Splitting of the Velocity into Acoustic, Entropic and Vortical Modes

$$\vec{V}(\vec{x},t) = \vec{U} + \vec{u}(\vec{x},t)$$

$$\frac{D_0}{Dt}\rho' + \rho_0 \nabla \cdot \vec{u} = 0$$

$$\frac{D_0}{Dt}\vec{u} + \rho_0 \nabla \cdot p' = 0$$

$$\vec{u} = \vec{u}_v + \nabla \phi$$

$$\frac{D_0}{Dt}\vec{u}_v = 0$$

$$\left(\frac{1}{c_0^2}\frac{D_0^2}{Dt^2} - \nabla^2\right)\phi = 0$$

$$\frac{D_0}{Dt}s' = 0$$

$$\frac{D_0}{Dt} \equiv \frac{\partial}{\partial t} + \vec{U}.\nabla$$

$$p' = -\rho_0 \frac{D_0}{Dt}\phi$$

Equations for Linear Aerodynamics

- Vortical Mode: $$\vec{u}_v = \vec{u}_\infty(\vec{x} - \vec{U}i)$$
  - Harmonic Component $$\vec{u}_g = \vec{a}e^{i(\vec{k}\cdot\vec{x} - \omega t)}$$
- Potential Mode: $$\left(\frac{1}{c_0^2}\frac{D_0^2}{Dt^2} - \nabla^2\right)\phi = 0$$
- Boundary Conditions: impermeability along blade surface, Kutta condition at trailing edge, allow for wake shedding in response to gust.

Flat Plate in a Gust

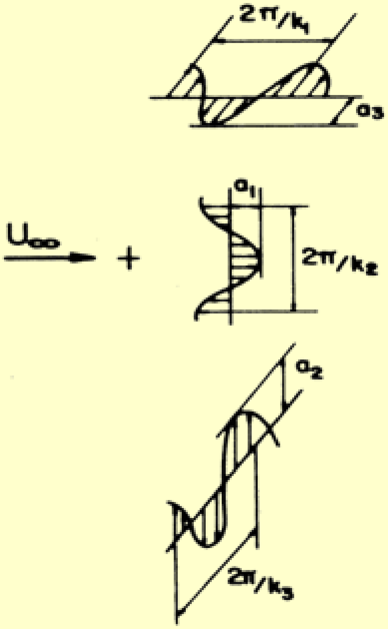

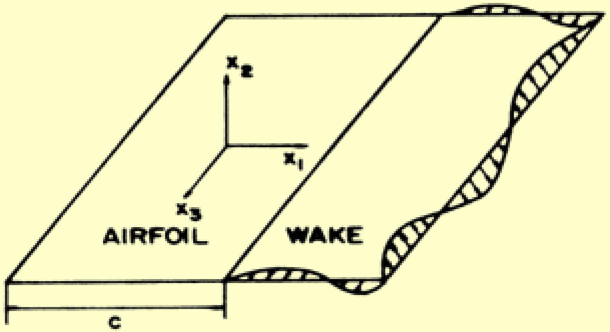

$$\vec{u}_g = \vec{a} e^{i(\vec{k}\cdot\vec{x} - \omega t)}$$

Transverse Gust: $(0,a_2,0)$, $(k_1,0,0)$

Oblique Gust: $(0,a_2,0)$, $(k1,0,k3)$

Vector Diagram Showing the Real and Imaginary Parts of the Response Function $S(k_1,0,M)$ versus k_1 for a Transverse Gust at Various M

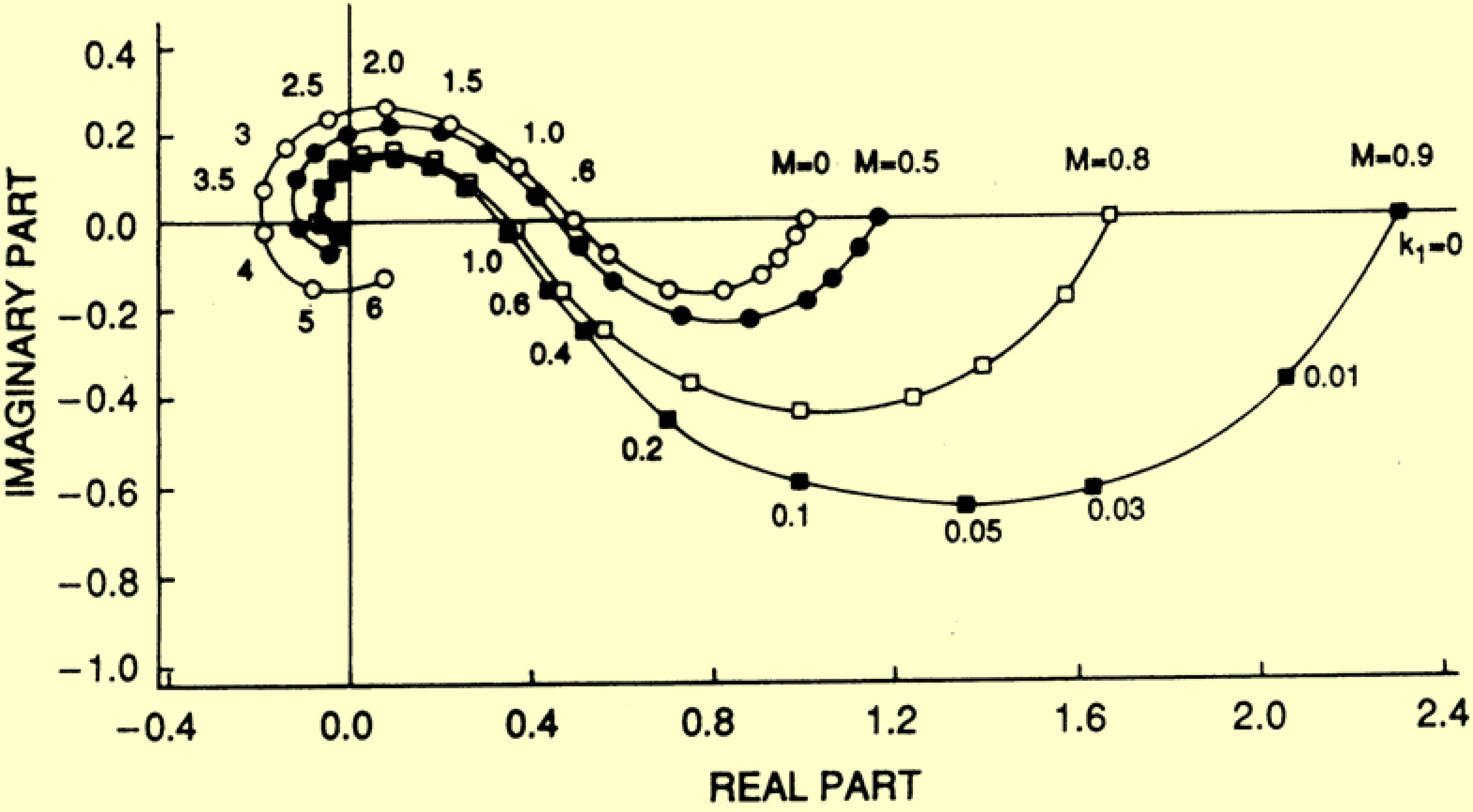

Vector Diagram Showing the Real and Imaginary Parts of the Response Function $S(k_1,k_3,0.8)$ versus k_1 for a Transverse Gust at Various M

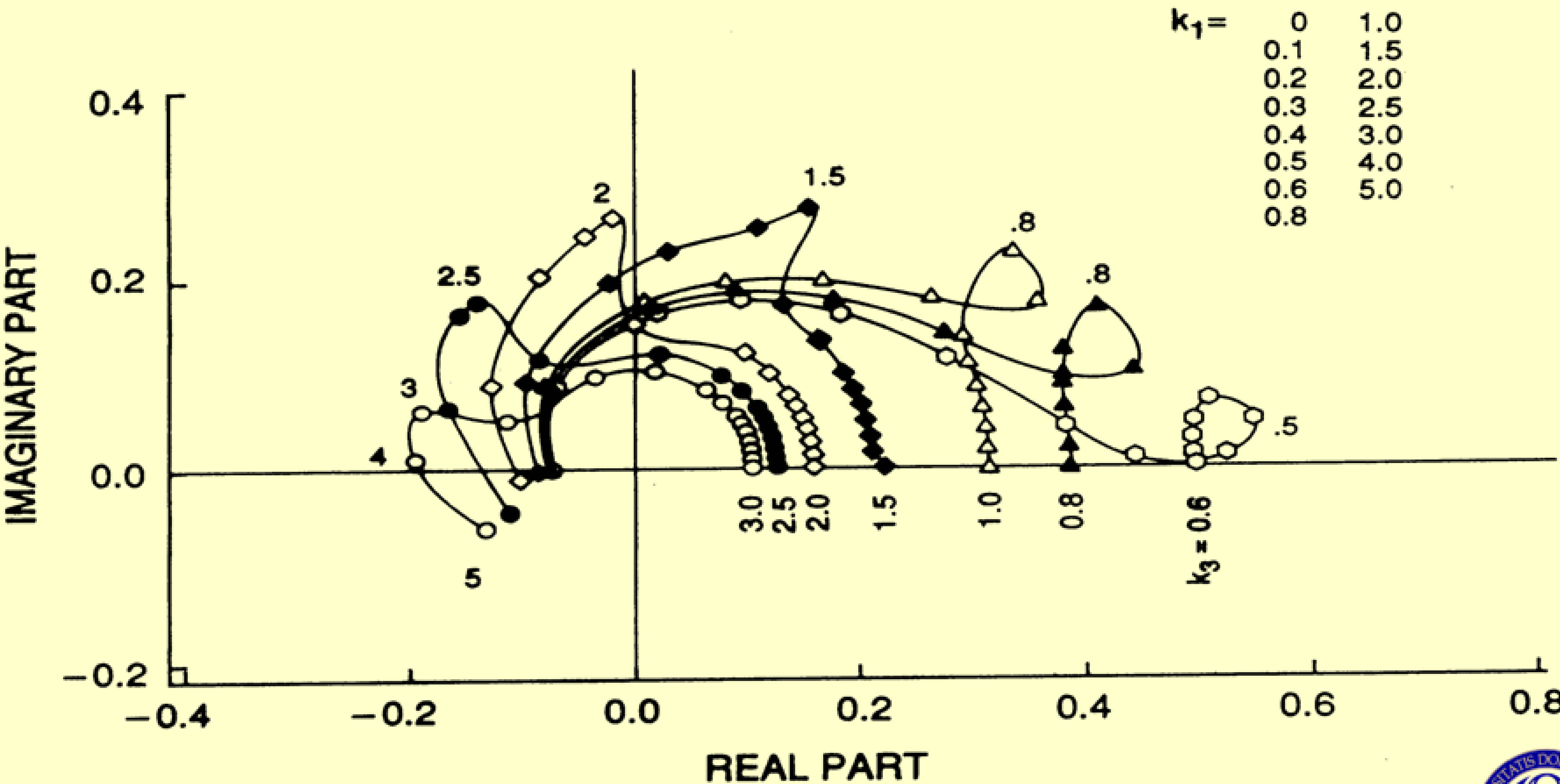

Airfoil in Three-Dimensional Gust

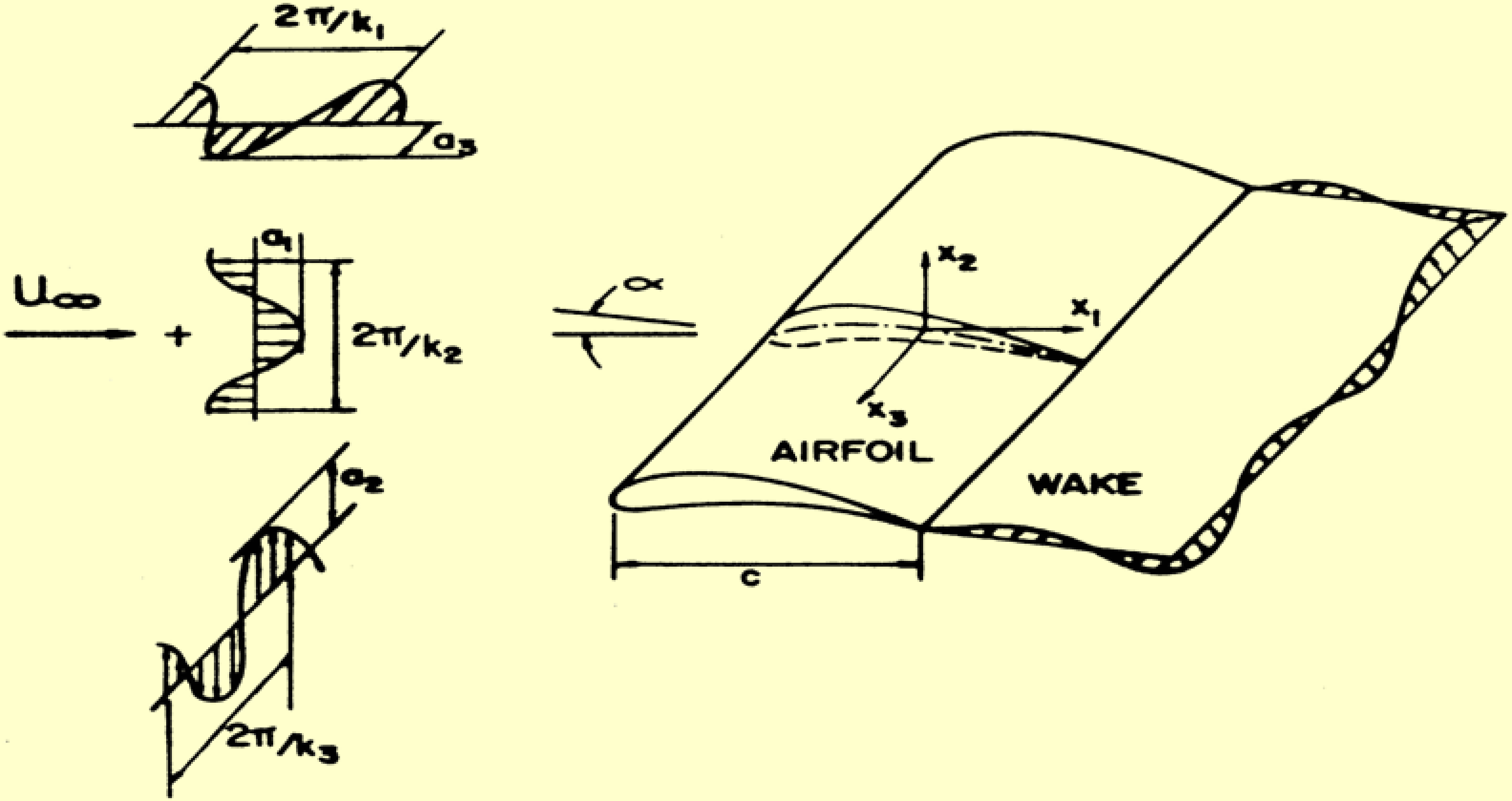

VORTEX STRETCHING AT THE STAGNATION POINT

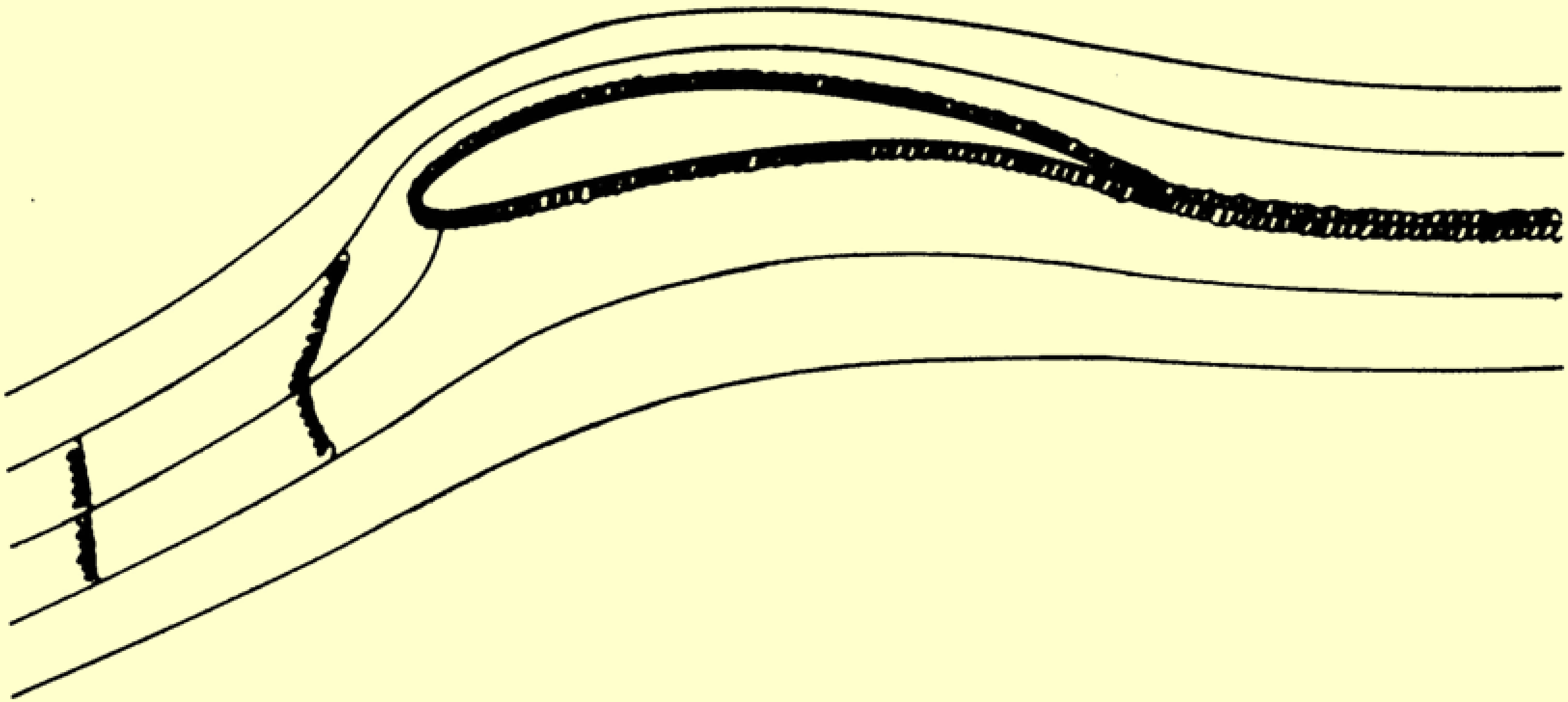

Vector Diagram Showing the Real and Imaginary Parts of the Response Function $S(k_1,k_2,k_3)$ versus k_1 for an Airfoil in an Oblique Gust ($k_2=k_1$) at Various k_3.

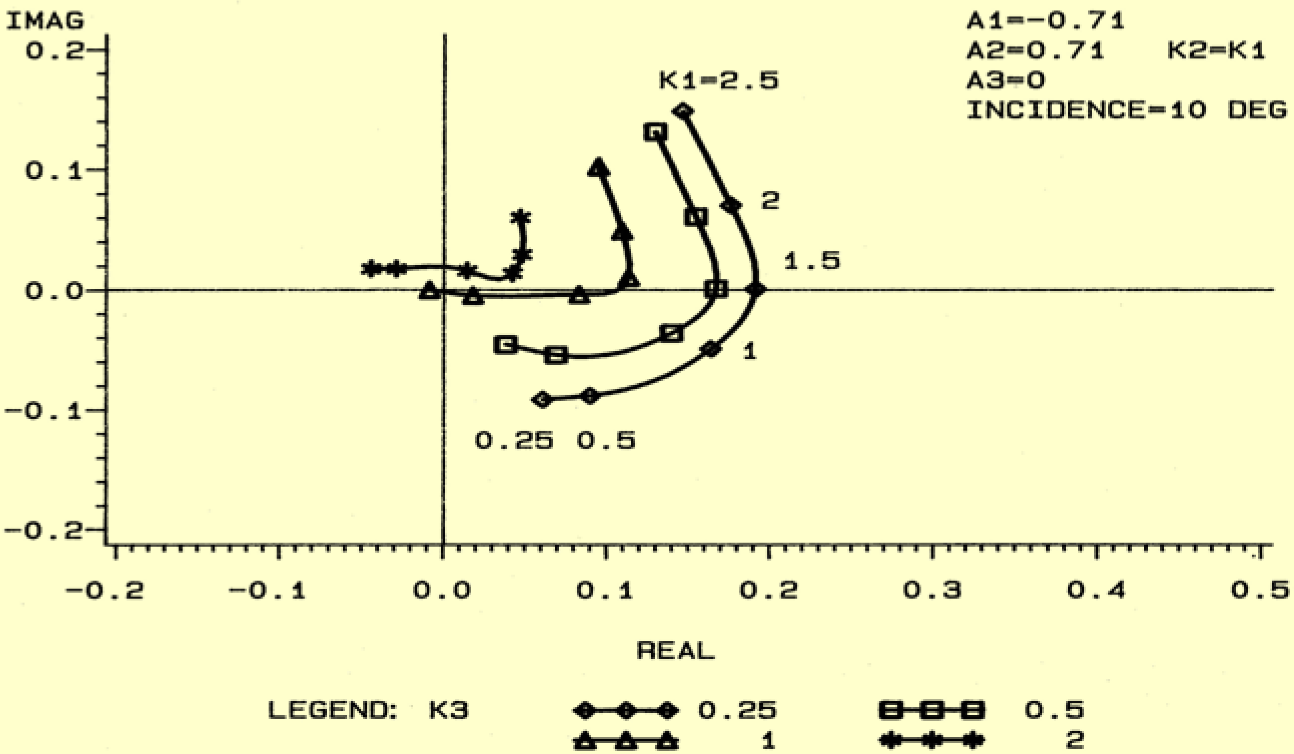

THE UNSTEADY LIFT COEFFICIENT
JOUKOWSKI AIRFOIL: CAMBER=0.1 THICKNESS=0.1

Acoustic Directivity for a 3% Thick Airfoil in a Transverse Gust at M=0.1, k_1=1.0

-.-, direct calculation from Scott-Atassi's code; —, Kirchhoff's method;---, flat plate semi-analytical results.

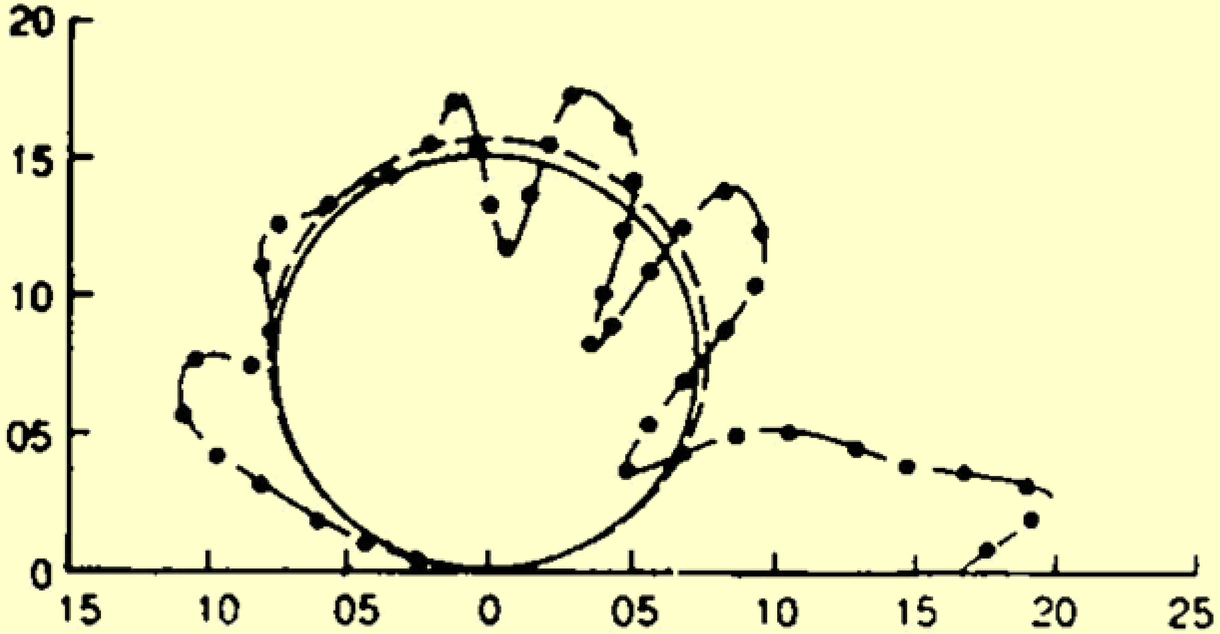

Acoustic Pressure Directivity for a Symmetric Airfoil in a Two-Dimensional Gust

Thichness Ratio=0.06, M=0.7, k_1=3.0

k_2: solid line,0.0; ------,3.0.

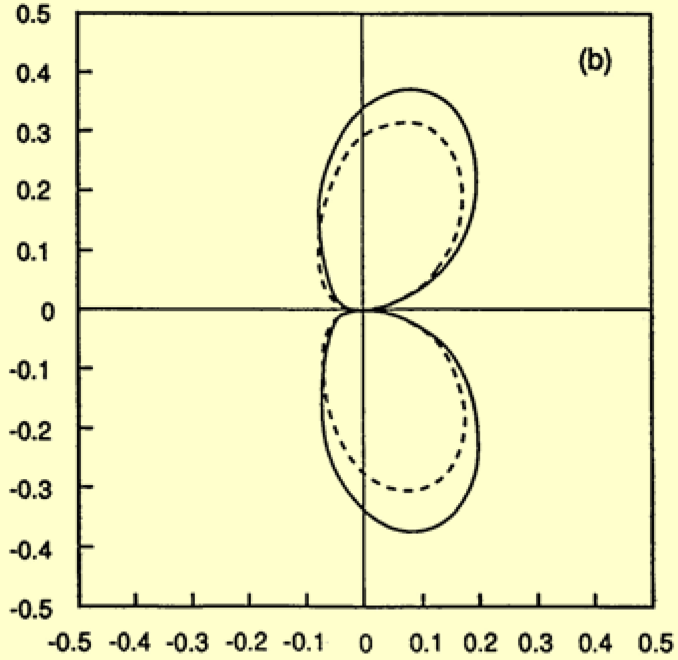

Dipole Acoustic Pressure

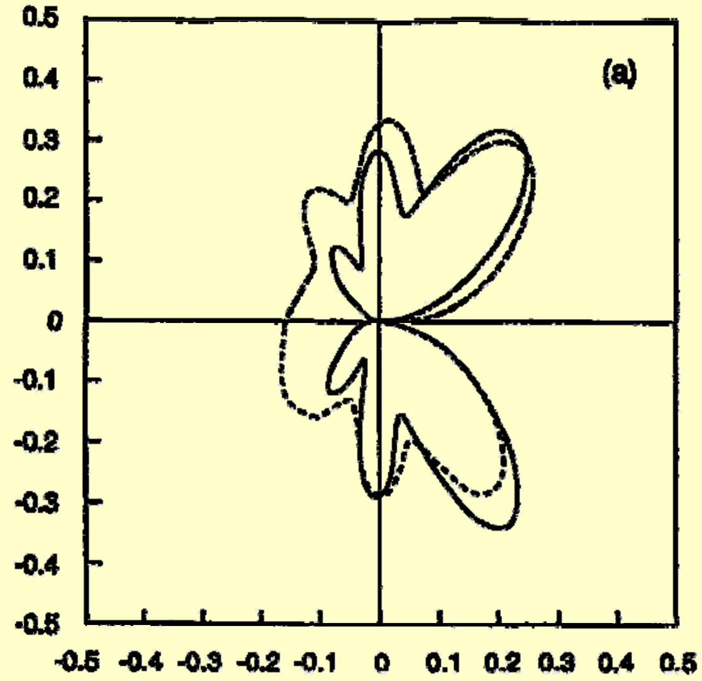

Total Acoustic Pressure

Acoustic Pressure Directivity for a Lifting Airfoil in a transverse Gust

Thichness Ratio=0.12, M=0.5, k_1=2.5

Camber: solid line,0.0; ------,0.2; -- . --, 0.4.

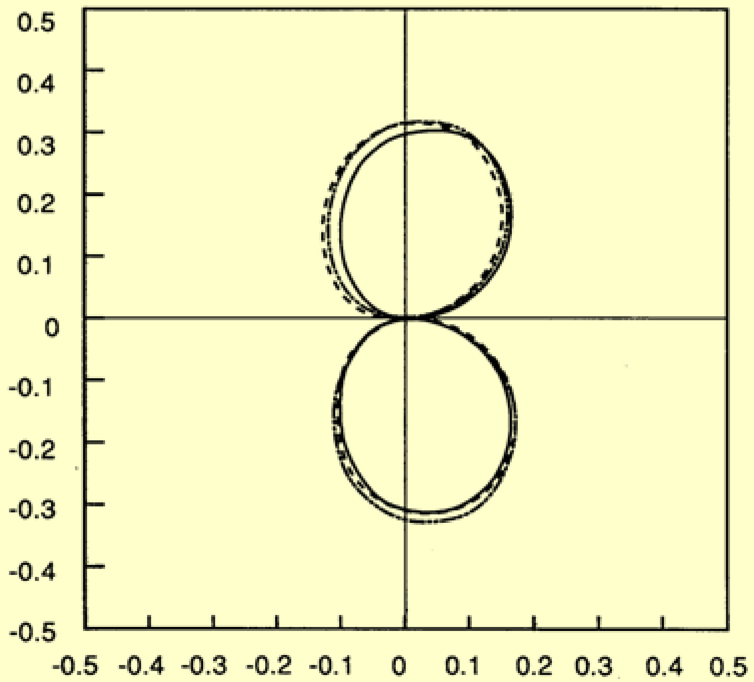

Dipole Acoustic Pressure

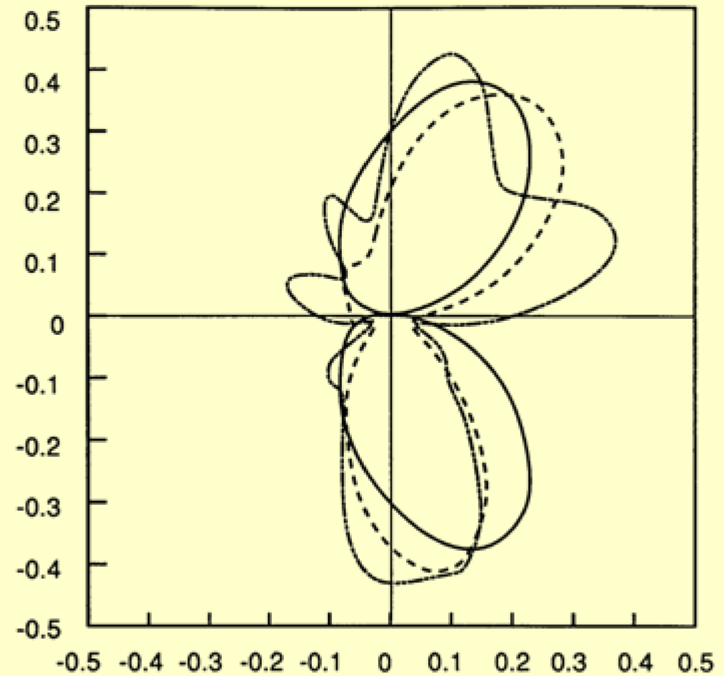

Total Acoustic Pressure

Conclusions

- At low Mach number, low frequency, dipole effects (unsteady airfoil pressure) dominate the scattered sound.
- At moderate and high Mach number and/or high frequency, the scattered sound strongly depends on both dipole and quadrupole effects and sound directivity is characterized by lobe formation.
- Loading strongly affects the scattered acoustic energy.
- Exact nonreflecting boundary conditions are essential for obtaining accurate results particularly at high Mach number and reduced frequency.

The Linear Cascade Model

- Separate rotor and stator and consider each blade row separately.
- Unroll the annular cacade into a linear cascade of infinite blade to preserve periodicity.
- **Flat-plate cascade**: uniform mean flow, integral equation formulation in terms of plane waves. The current benchmark.
- **Loaded cascade**: Linearized Euler about a computationally calculated mean flow, requires field solutions of pde. CASGUST and LINFLOW are current benchmarks.

Unrolling of the Annular Cascade
The Linear Cascade

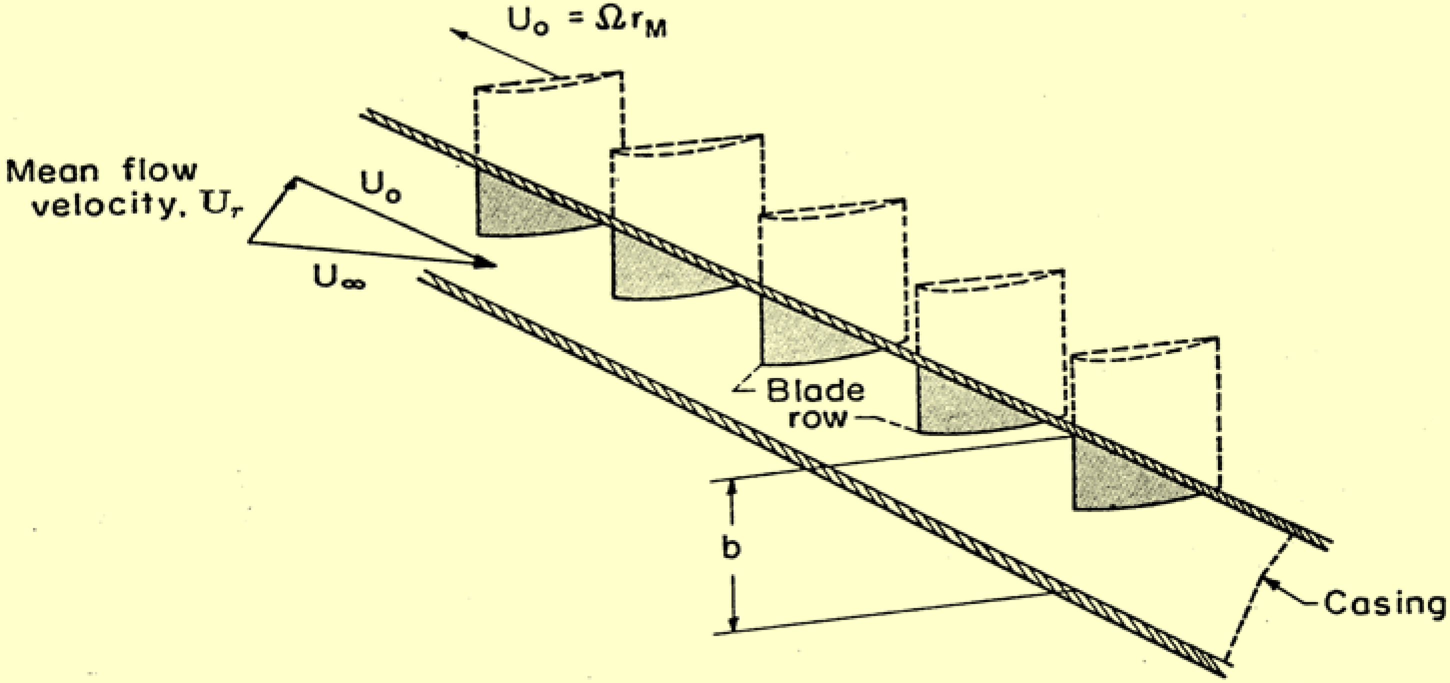

Linear Cascade and Strip Theory

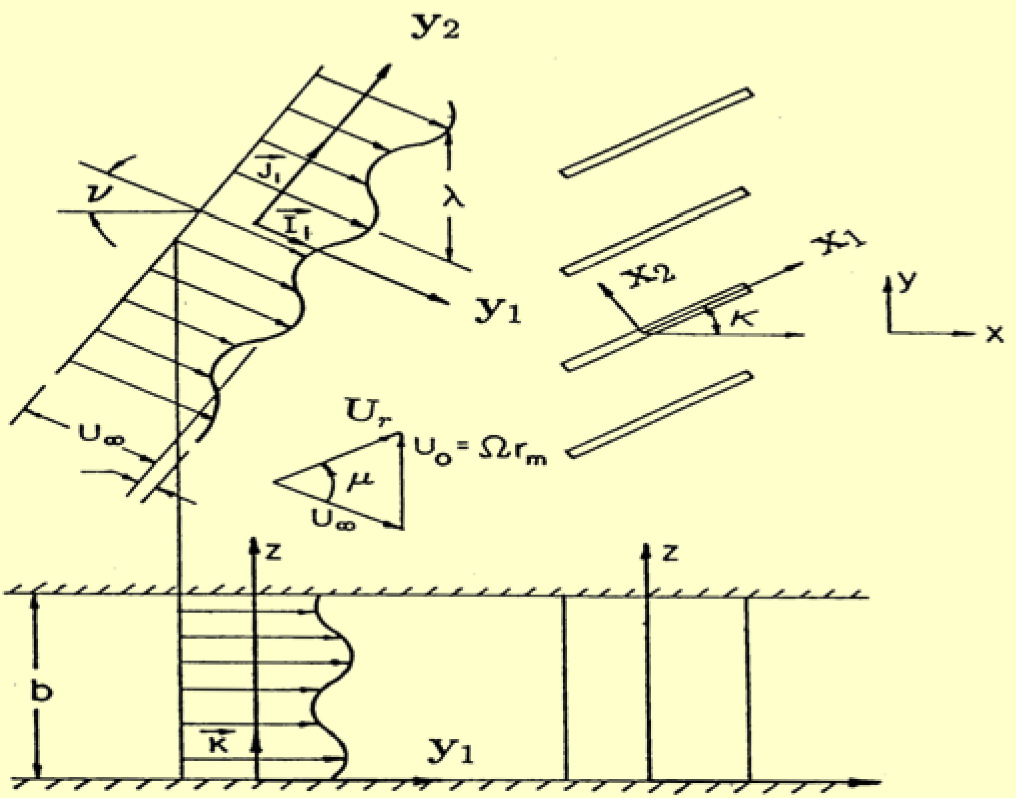

FLOW IN CASCADE

Cascade of Airfoils in a Three-Dimensional Gust

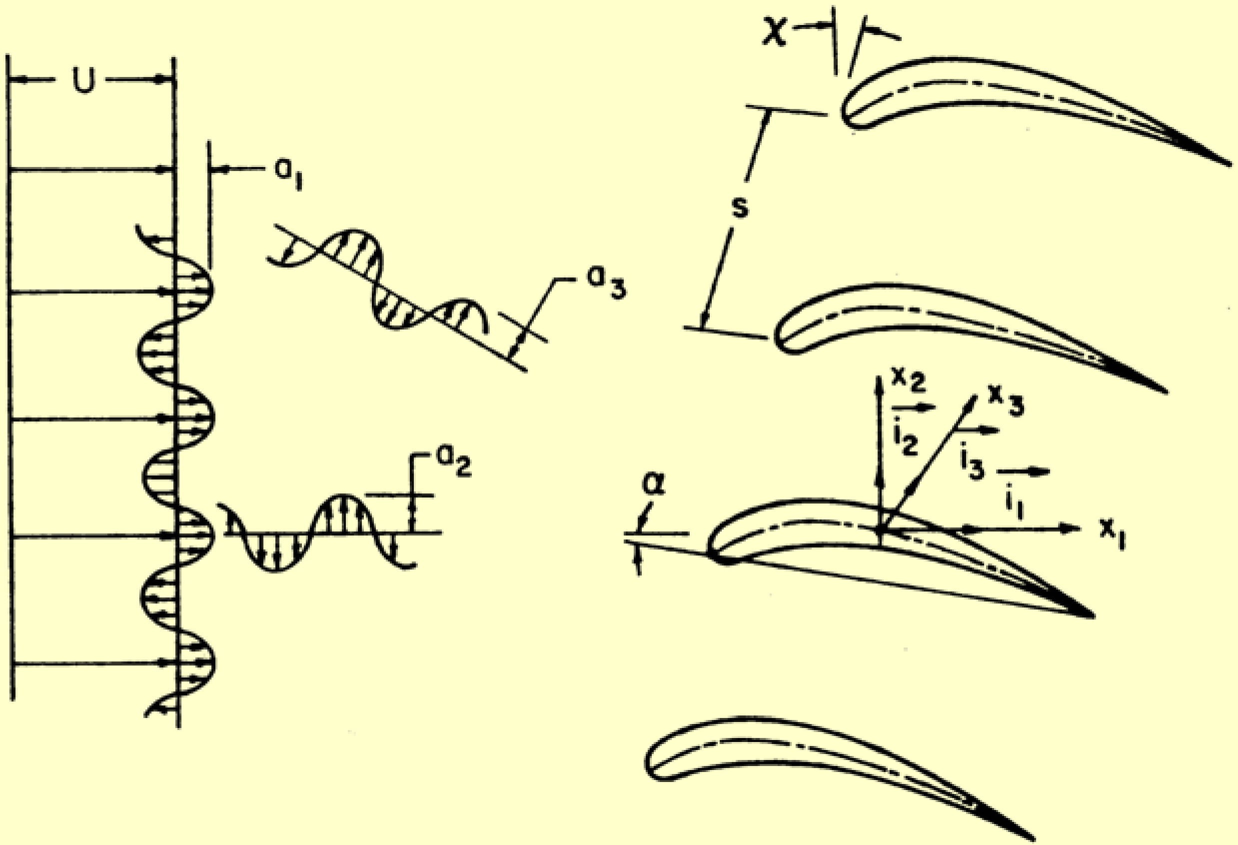

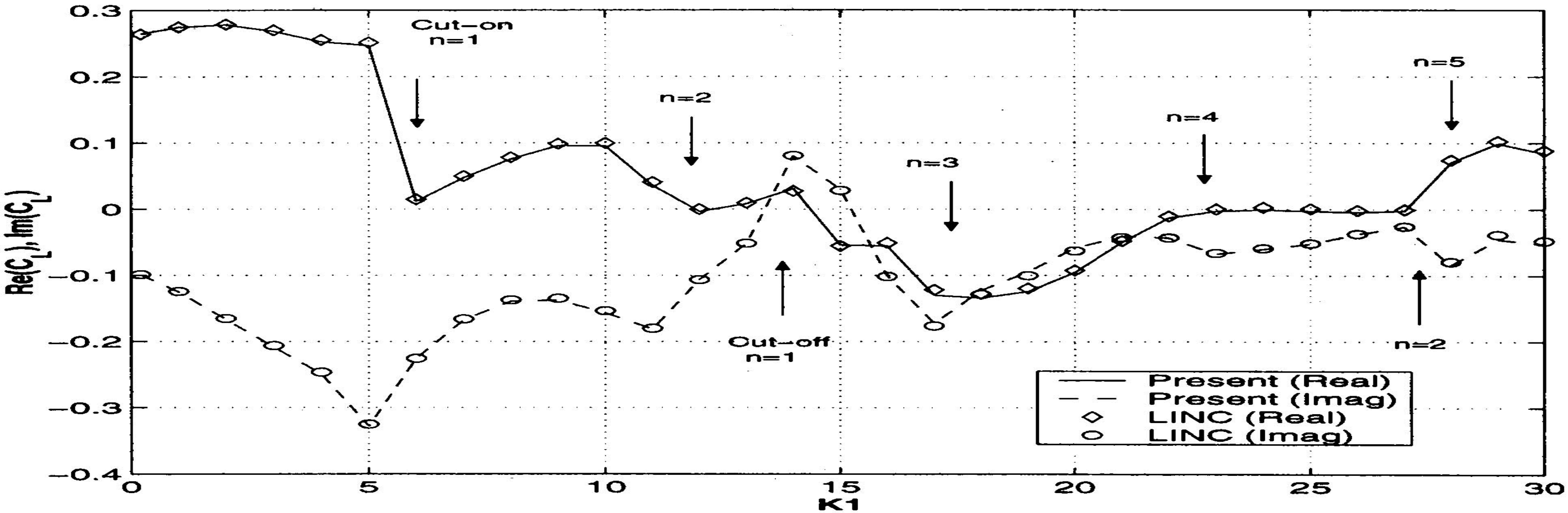

Figure 3: Real and imaginary parts of the unsteady lift versus the reduced frequency k_1 for a cascade of flat plates ($\chi = 45^o$, $\frac{S}{c} = 1.0$, $M_\infty = 0.3$, $k_2 = 0$)

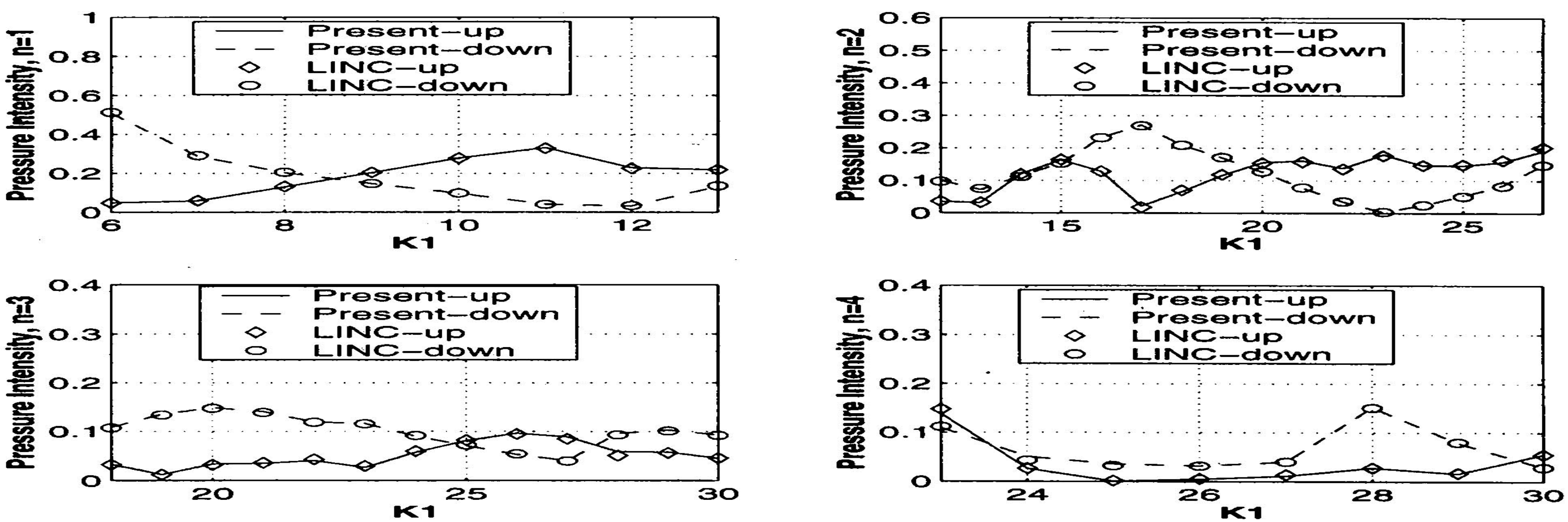

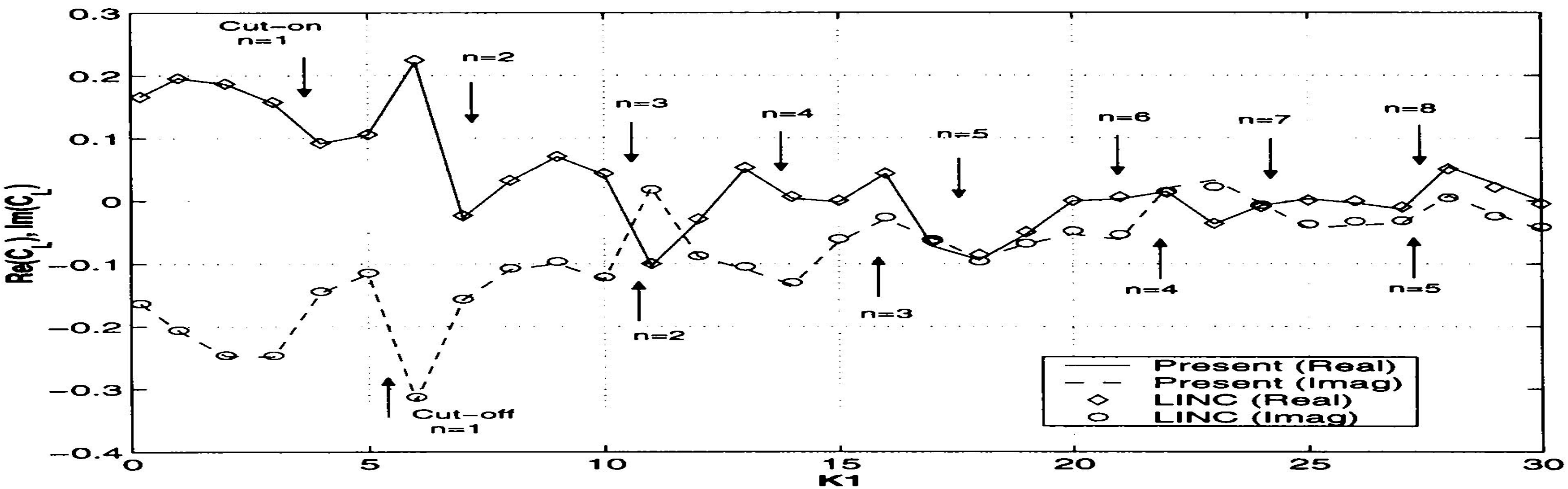

Figure 5: Real and imaginary parts of the unsteady lift versus the reduced frequency k_1 for a cascade of flat plates ($\chi = 45^o$, $\frac{S}{c} = 1.0$, $M_\infty = 0.3$, $k_2 = k_1$)

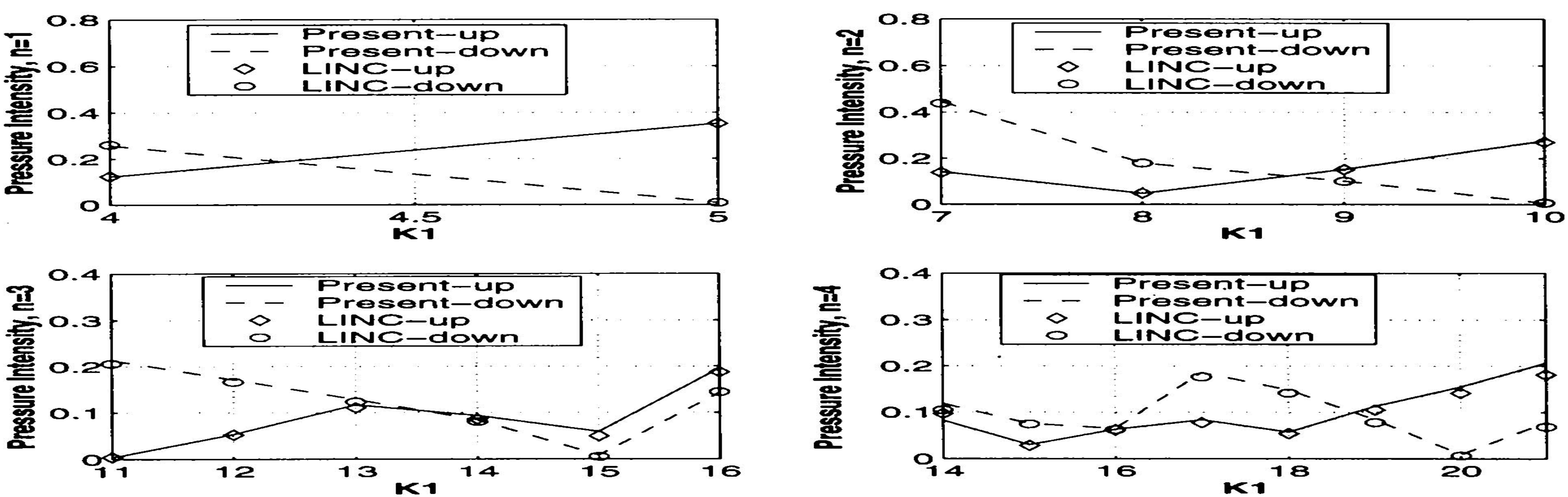

Figure 6: The first four modes of the sound radiated from a cascade of flat plates ($\chi = 45^o$, $\frac{S}{c} = 1.0$, $M_\infty = 0.3$, $k_2 = k_1$)

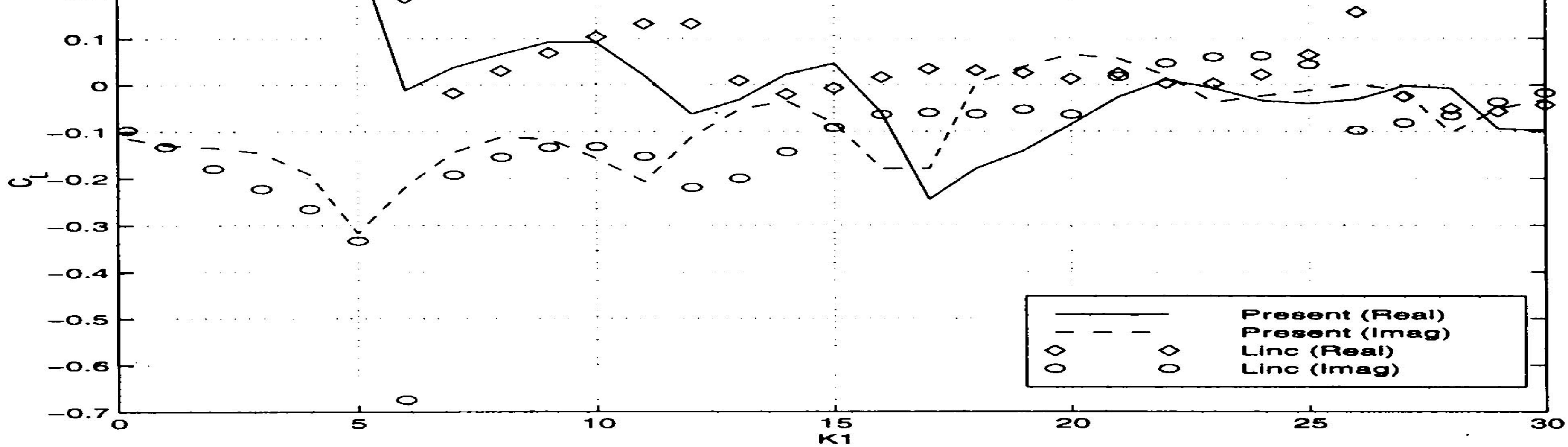

Figure 11: Real and imaginary parts of the unsteady lift versus the reduced frequency k_1 for a cascade of NACA 4406 blades ($\chi = 35^o$, $\frac{S}{c} = 1.0$, $M_\infty = 0.3$, $k_2 = 0$)

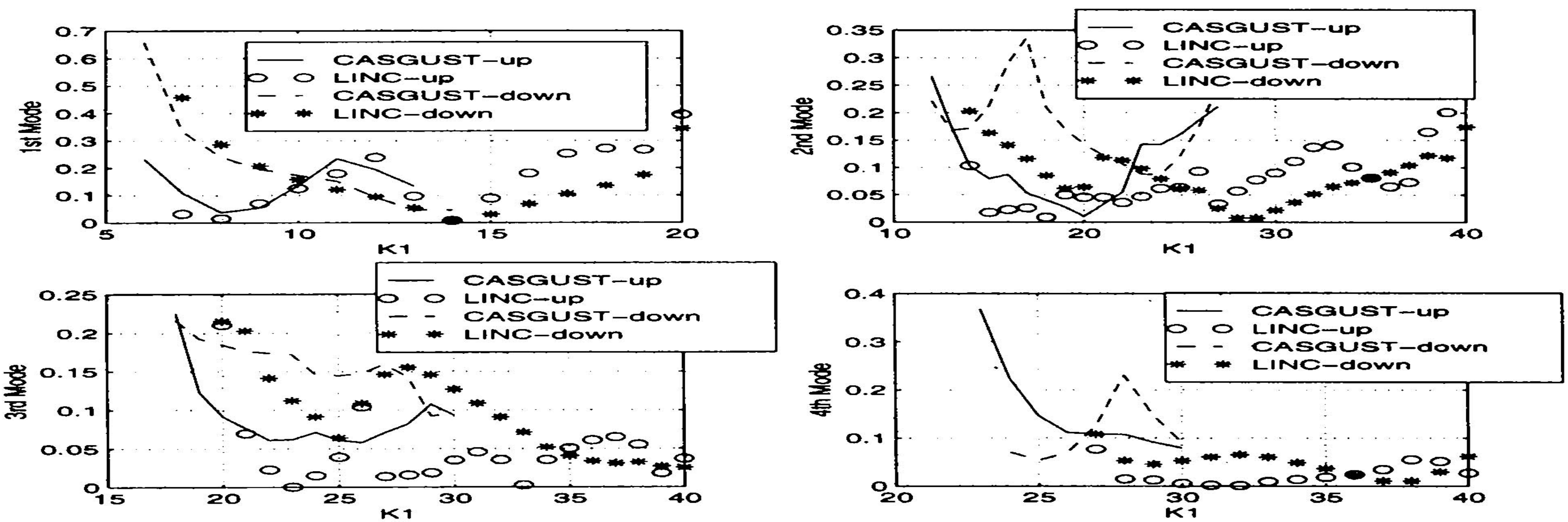

Figure 12: The first four modes of the sound radiated from a cascade of NACA 4406 blades ($\chi = 35^o$, $\frac{S}{c} = 1.0$, $M_\infty = 0.3$, $k_2 = 0$)

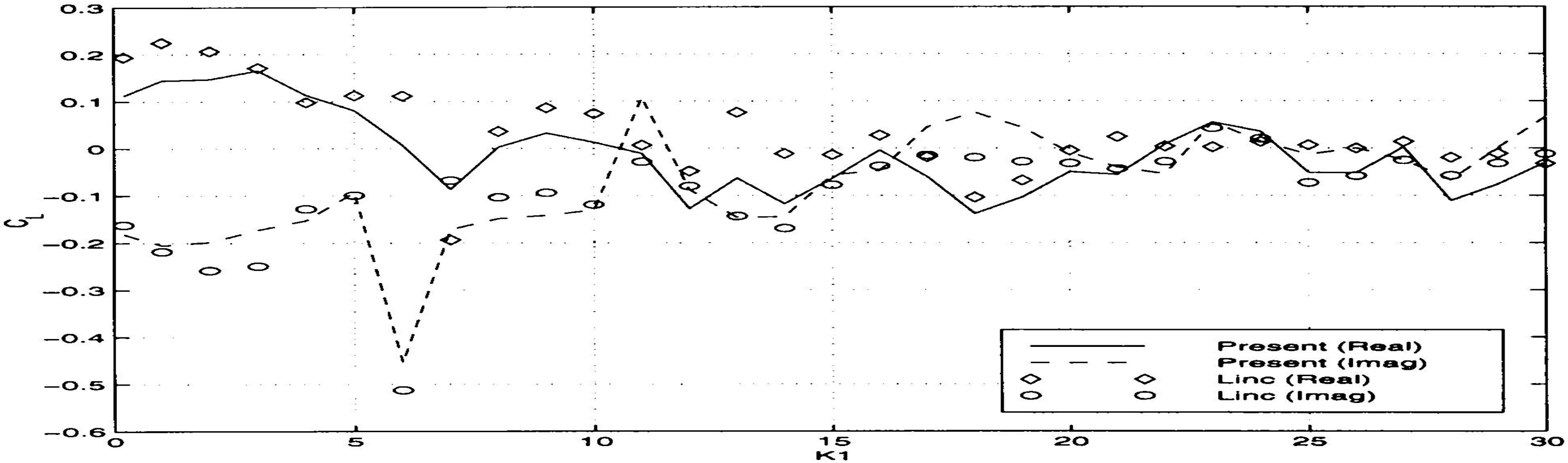

Figure 13: Real and imaginary parts of the unsteady lift versus the reduced frequency k_1 for a cascade of NACA 4406 blades ($\chi = 35^o$, $\frac{S}{c} = 1.0$, $M_\infty = 0.3$, $k_2 = k_1$)

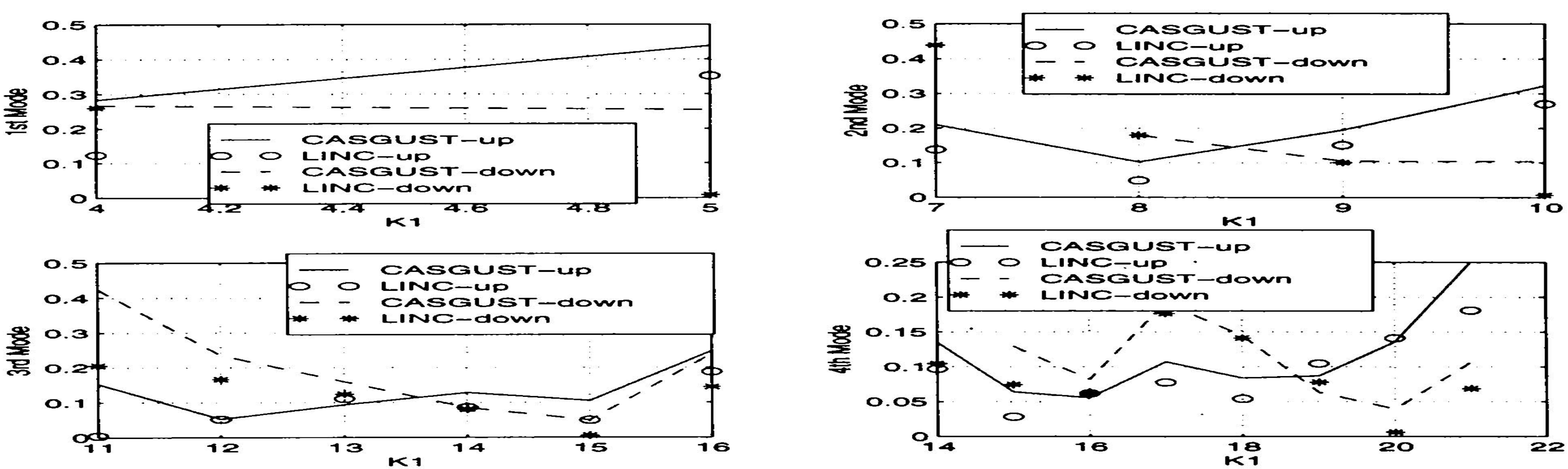

Figure 14: The first four modes of the sound radiated from a cascade of NACA 4406 blades ($\chi = 35^o$, $\frac{S}{c} = 1.0$, $M_\infty = 0.3$, $k_2 = k_1$)

Magnitude of the Response Function S versus k1 for an EGV Cascade(squares) with Flat-Plate Cascade(circles). M=0.3, k2=k1

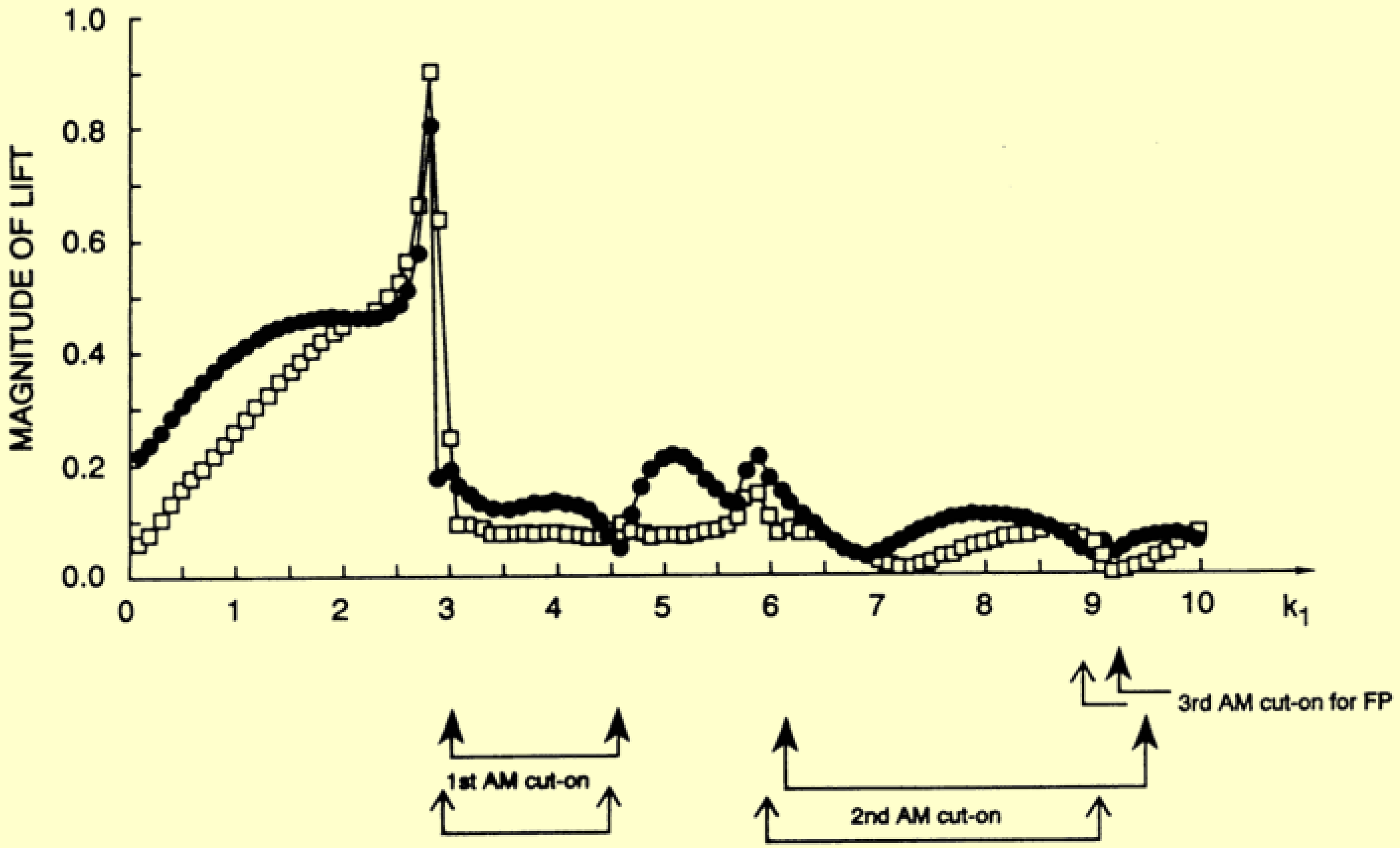

Magnitude of the Downstream Acoustic Modes fro an EGV Cascade with Those of a Flat Plate Cascade(solid)

M=0.3, k2=k1

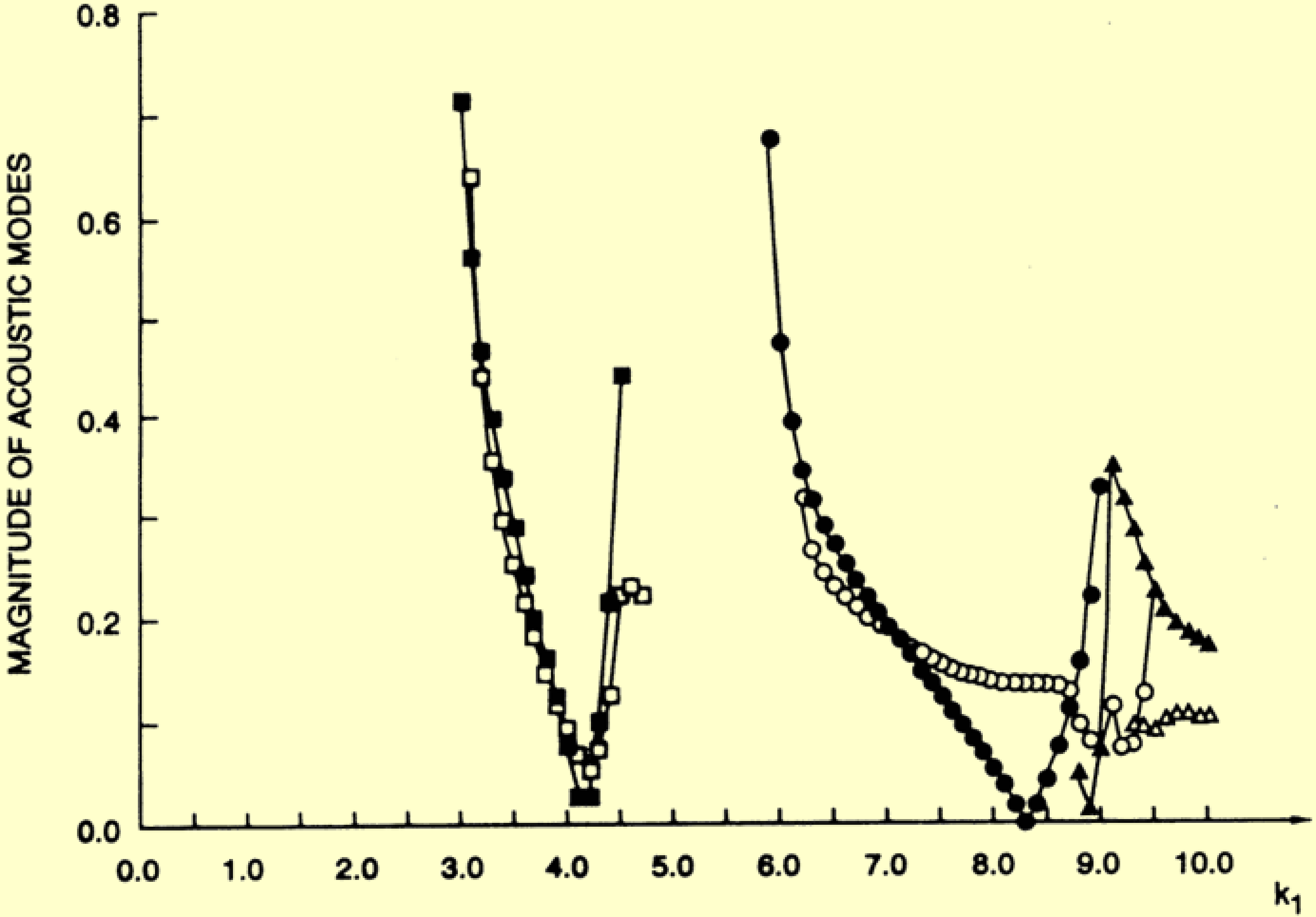

How Good is the Linearized Euler Model?

Cascade Flow with local Regions of Strong Interaction

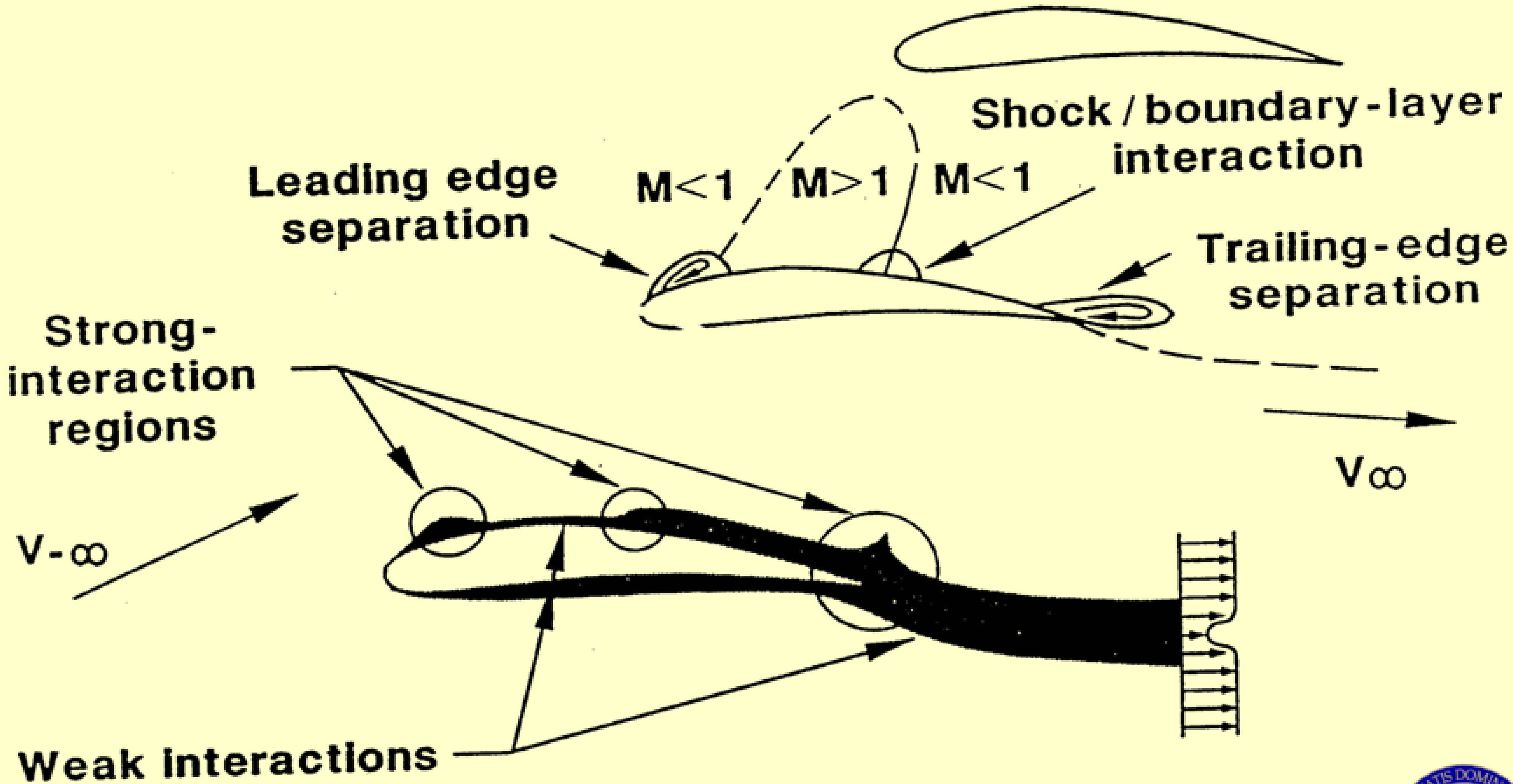

COMPRESSOR EXIT GUIDE VANE

NGUST Computational Grid

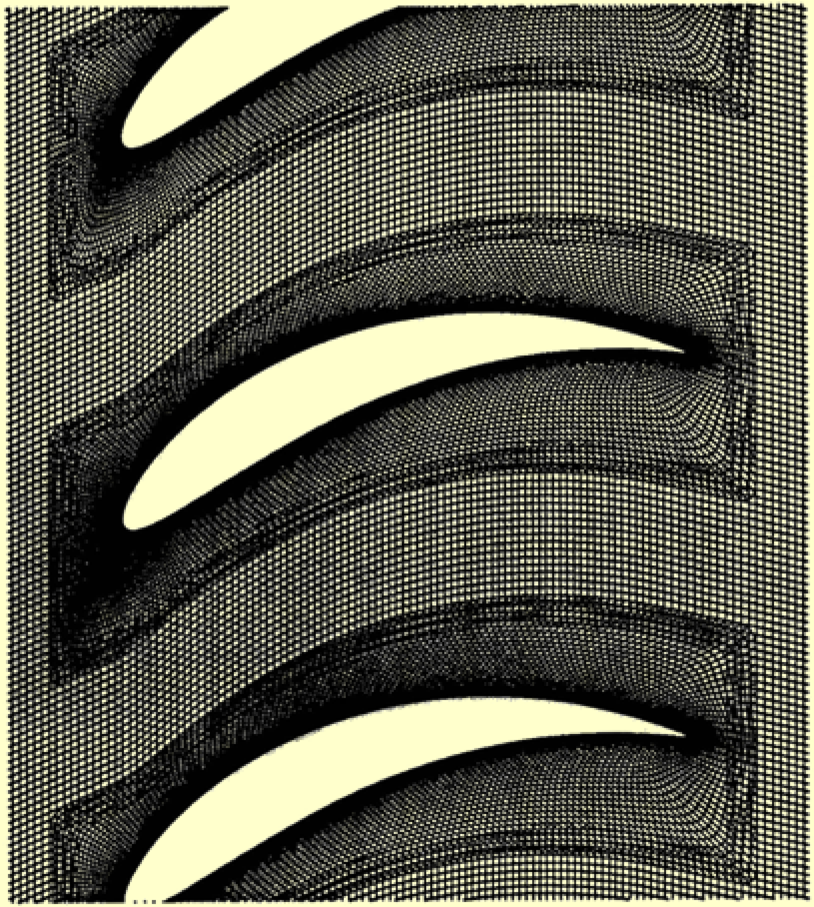

HIGH SPEED COMPRESSOR CASCADE

Surface Mach Number Distributions

—— Potential, - - - -- Euler

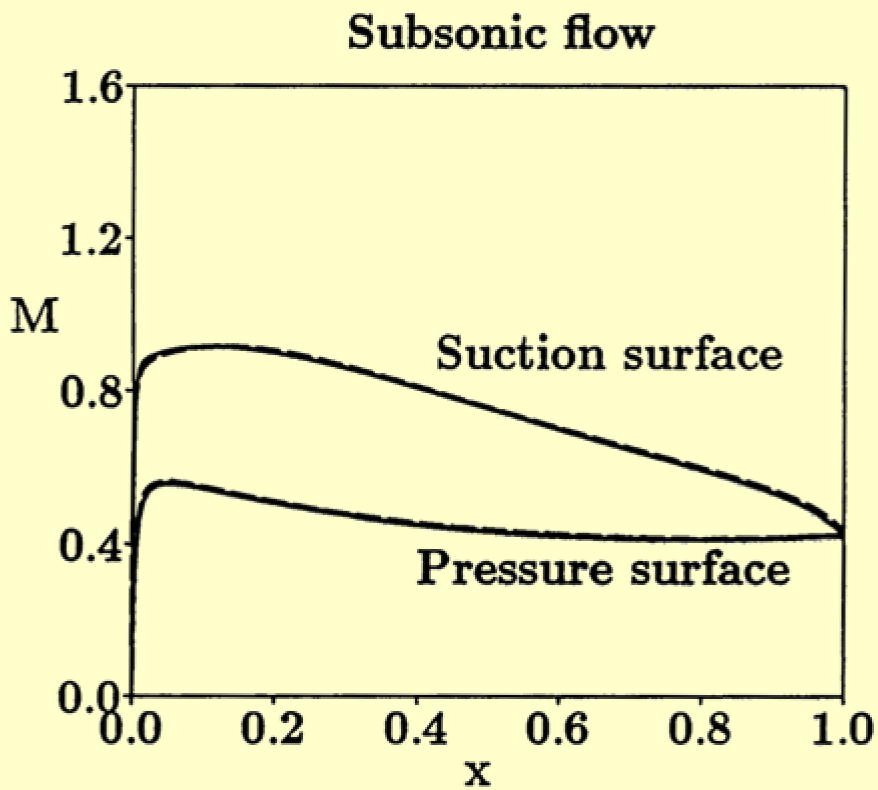

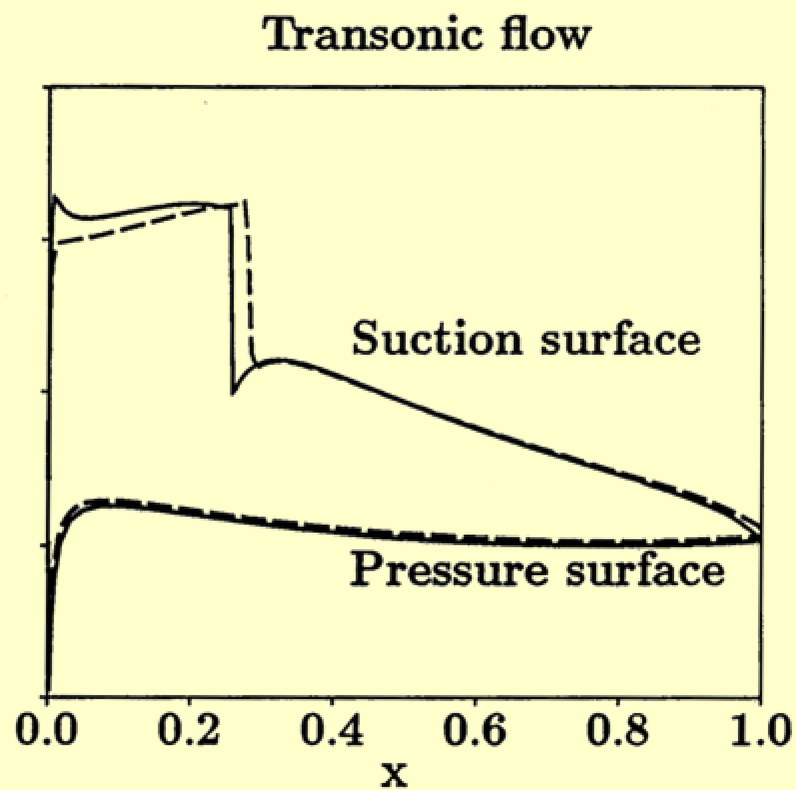

Magnitude (a) and Phase (b) of the first Harmonic Unsteady Pressure Difference Distribution for the subsonic NACA 0006 Cascade Underhoing an In-Phase Torsional Oscillation of Amplitude a=2o at k1=0.5 about Midchord; M=0.7; —,Linearized Analysis; ....Nonlinear Analysis.

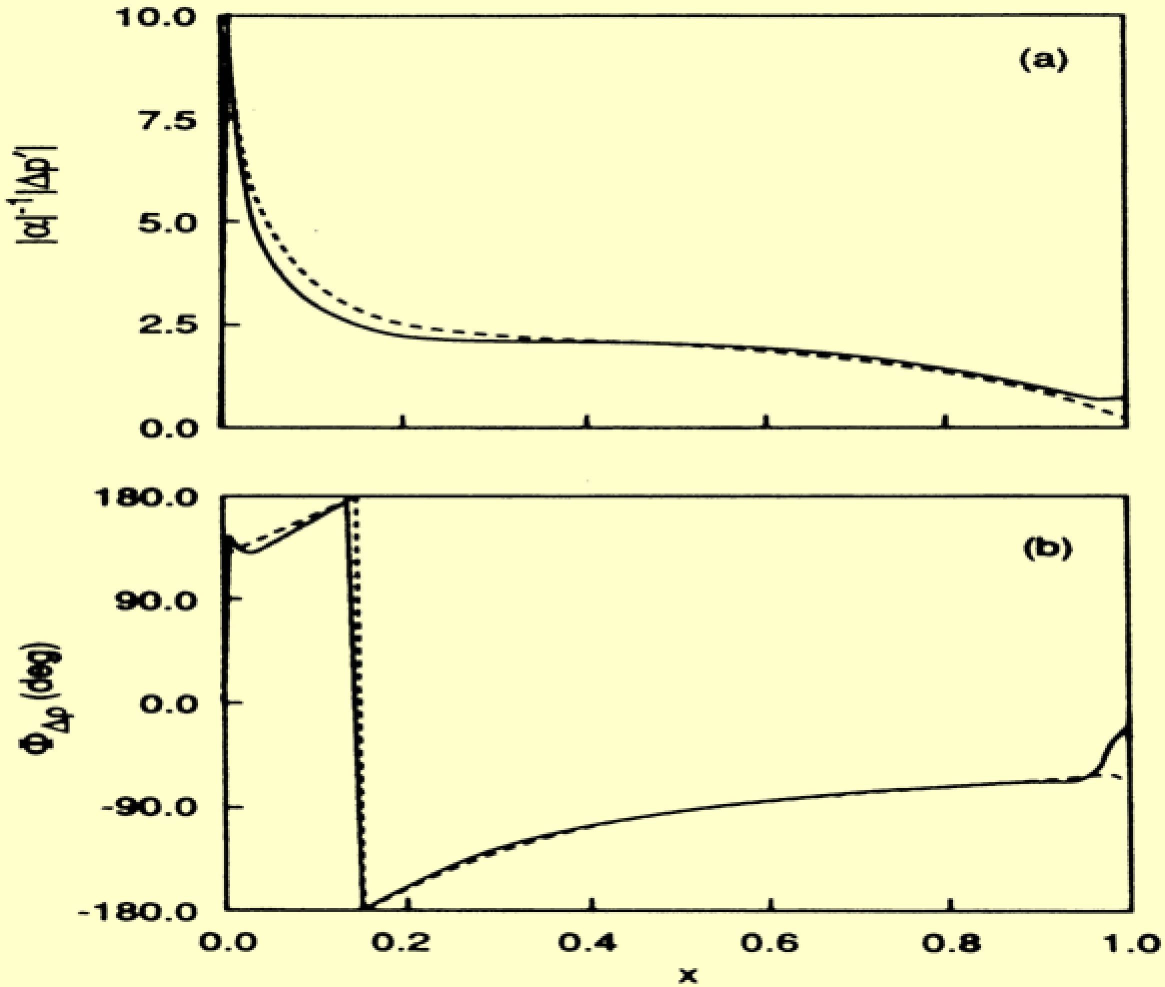

Magnitude (a) and Phase (b) of the first Harmonic Unsteady Pressure Difference Distribution for the subsonic NACA 0006 Cascade Underhoing an In-Phase Torsional Oscillation of Amplitude a=2o at k1=0.5 about Midchord; M=0.7.

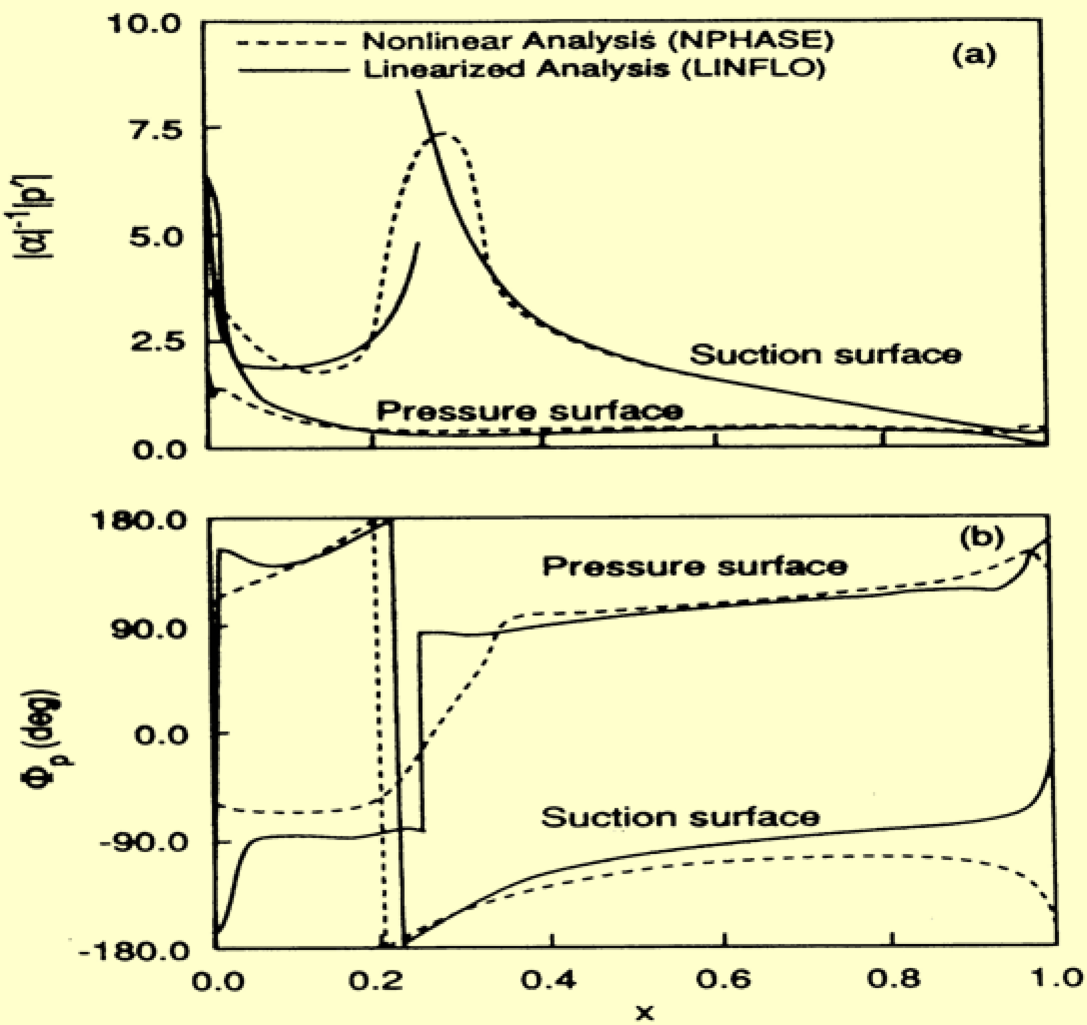

Conclusions

- Cascade effects such as blade interference which depends on the spacing ratio, and stagger have strong influence on the aerodynamic and acoustic cascade response, particularly at low frequency.
- At high frequency the cascade response is dominated by the acoustic modes cut-on phenomena.
- For thin blades, the leading edge dominates the aerodynamic pressure and noise generation.
- For loaded blades at high Mach number, large unsteady pressure excitations spread along the blade surface with concentration near the zone of transonic velocity.
- Blade loading changes the upstream and downstream flows and thus affects the number and intensity of the scattered sound.

Recent Developments in Fan Modeling

- **Tonal and Broadband Noise**
- **Nonuniform Mean Flow Effects :swirl**
- **Three-Dimensional Effects**
- **High Frequency Effects**

Tonal and Broadband

- Turbulence modeling using the rapid distortion theory.
- Hanson (Pratt & Whitney), Glegg (Florida) developed models using linear flat-plate cascades.
- Effects of blade loading, 3D effects are under development at ND

Turbulence Representation

- Fourier representation:

$$\vec{u}(\vec{x},t) = \int_{\omega,\vec{k}} \vec{a}(\vec{k},\omega) e^{i(\vec{k}.\vec{x}-\omega t)} d\vec{k} d\omega$$

$$\overline{a_i(\vec{k}) a_j(\vec{k}')} = \Phi_{ij}(\vec{k}) \delta(\vec{k}-\vec{k}')$$

- Evolution of each Fourier component

$$u_i(\vec{x},t) = \mu_{ij}(\vec{x},\vec{k}) a_j e^{-ik_1 Ut}$$

- Velocity covariance

$$R_{ij}(\vec{x},\vec{x}',t) = \int_{\vec{k}} \mu^*_{ik}(\vec{x},\vec{k}) \mu_{j\ell}(\vec{x}',\vec{k}) \Phi^{(0)}_{k\ell}(\vec{k}) e^{-ik_1 Ut} d\vec{k}$$

- One-dimensional energy spectrum

$$\Theta_{ij}(\vec{x},\vec{x}',k_1) = \int_{-\infty}^{+\infty} \int_{-\infty}^{+\infty} \mu^*_{ik}(\vec{x},\vec{k}) \mu_{j\ell}(\vec{x}',\vec{k}) \Phi^{(0)}_{k\ell}(\vec{k}) dk_2 dk_3$$

Aerodynamic and Acoustic Blade Response

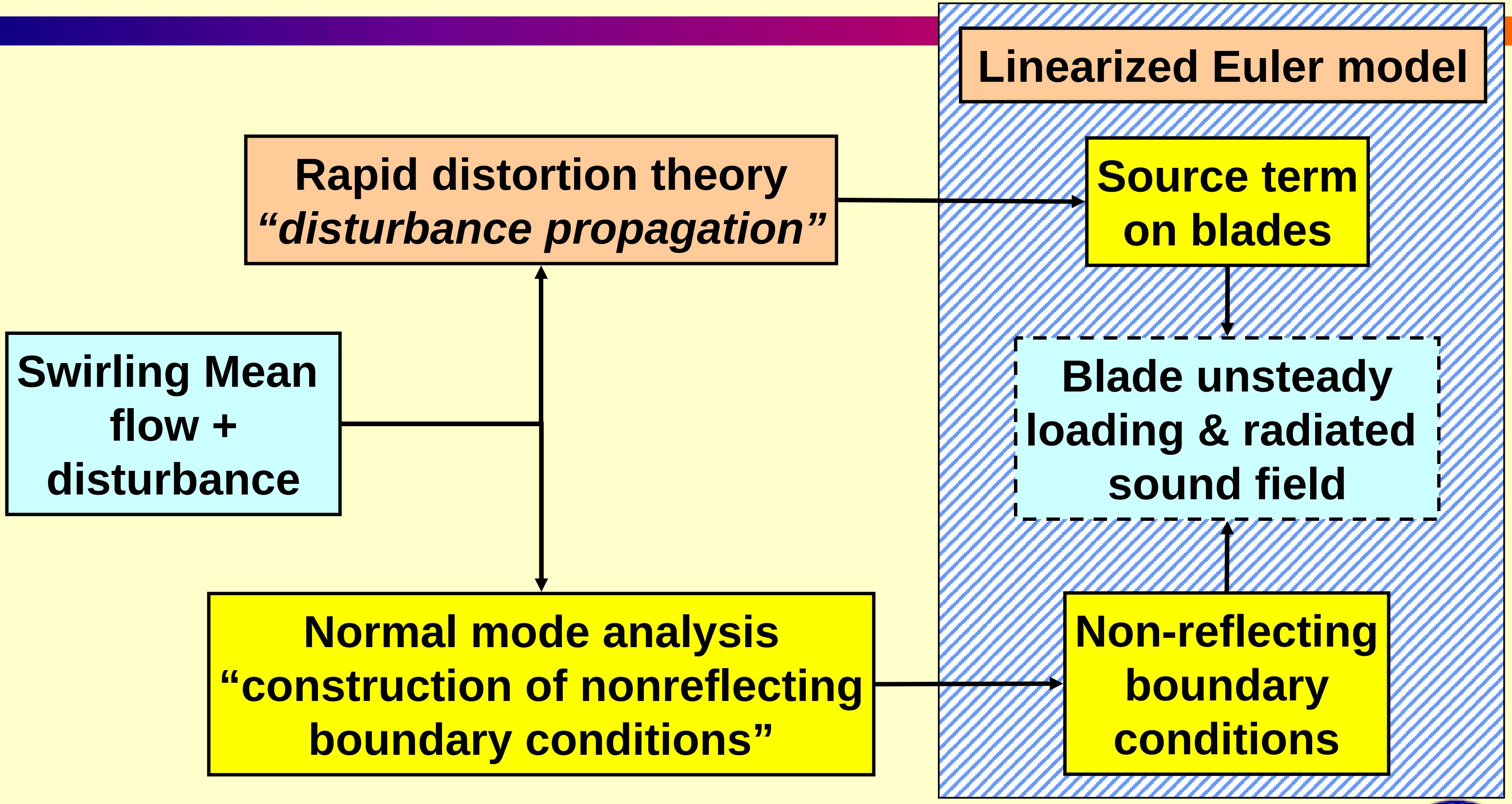

Mathematical Formulation

- Linearized Euler equations
- Axisymmetric swirling mean flow

$$\vec{U}(\vec{x}) = U_x(x,r)\vec{e}_x + U_s(x,r)\vec{e}_\theta$$

- Mean flow is obtained from data or computation
- For analysis the swirl velocity is taken

$$U_s = \Omega r + \frac{\Gamma}{r}$$

- The stagnation enthalpy, entropy, velocity and vorticity are related by Crocco's equation

$$\nabla H = T\nabla S + \mathbf{U} \times \zeta$$

Normal Mode Analysis

- A normal mode analysis of linearized Euler equations is carried out assuming solutions of the form
- $$\boxed{f(r)e^{i(-\omega t + m_{\nu}\theta + k_{mn}x)}}$$
- A combination of spectral and shooting methods is used in solving this problem
  - Spectral method produces spurious acoustic modes
  - Shooting method is used to eliminate the spurious modes and to increase the accuracy of the acoustic modes

$$\Lambda_{mn} = \frac{D_0}{Dt} = -\omega + k_{mn}U_x + \frac{mU_s}{r}$$

Mode Spectrum
Spectral and Shooting Methods

M_x=0.55, M_Γ=0.24, M_Ω=0.21, ω=16, and m=-1

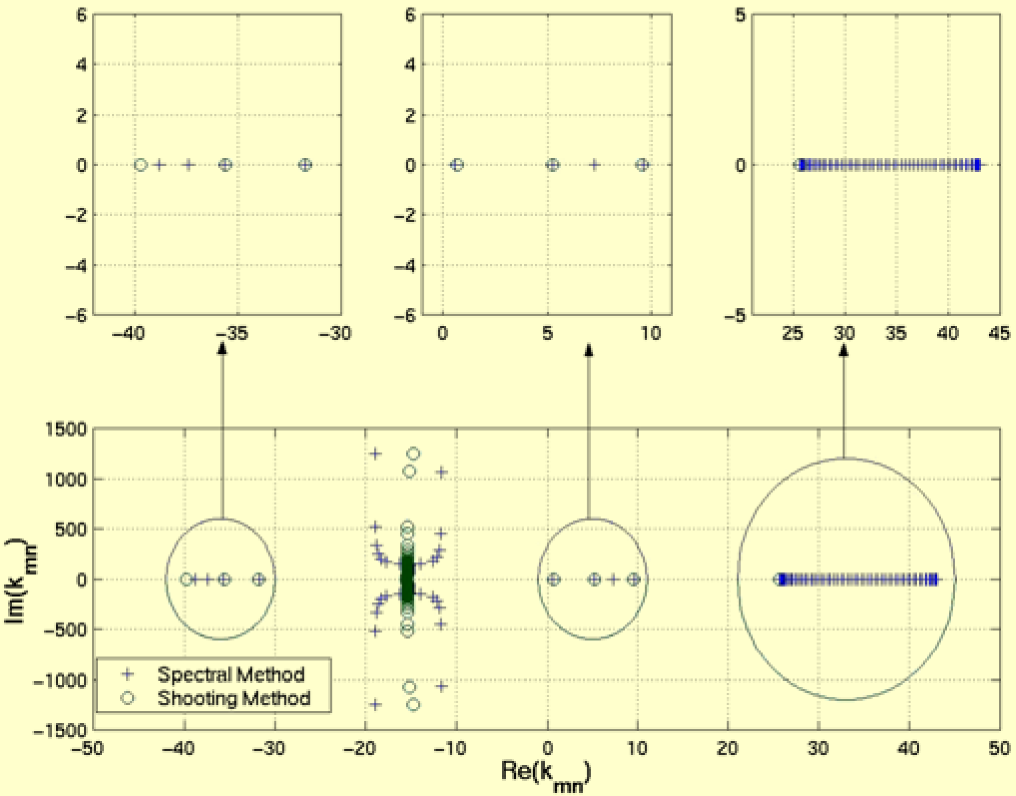

Pressure Content of Acoustic and Vortical Modes

M_x=0.5, M_Γ=0.2, M_Ω=0.2, ω=2π, and m=-1

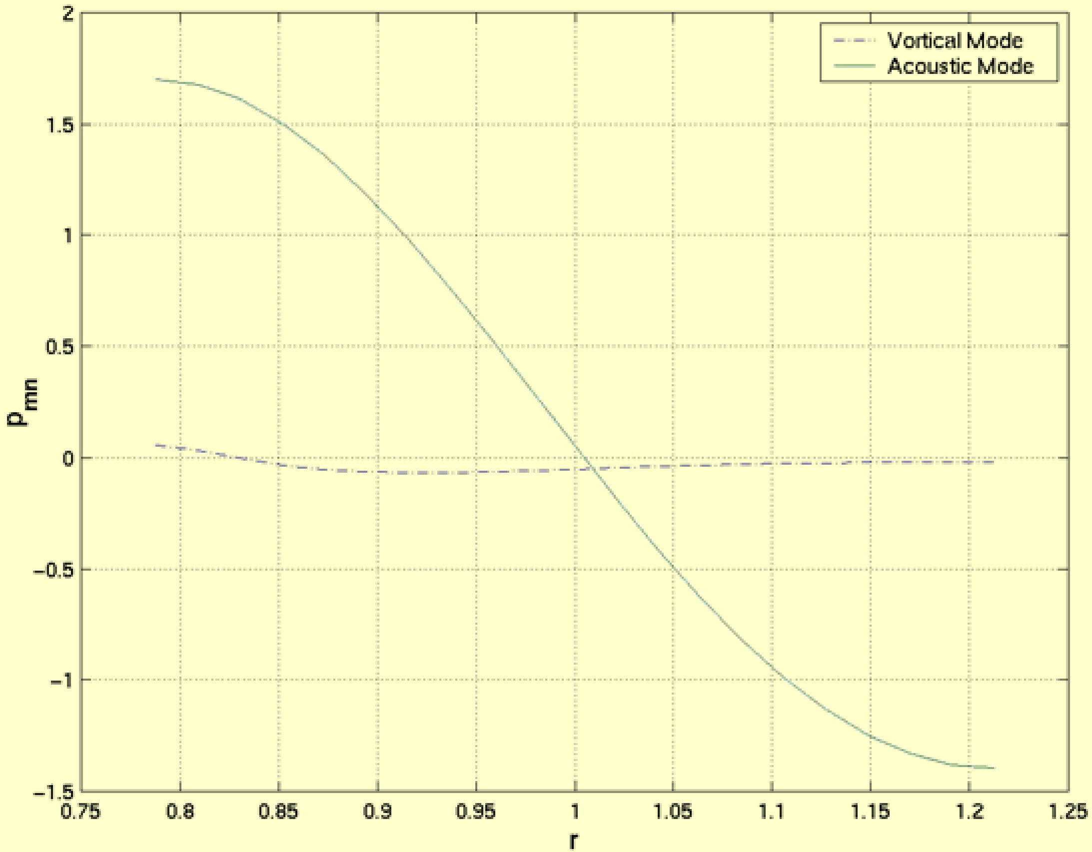

Effect of Swirl on Eigenmode Distribution

$M_{xm=}0.56$, $M_{\Gamma}=0.25$, $M_{\Omega}=0.21$

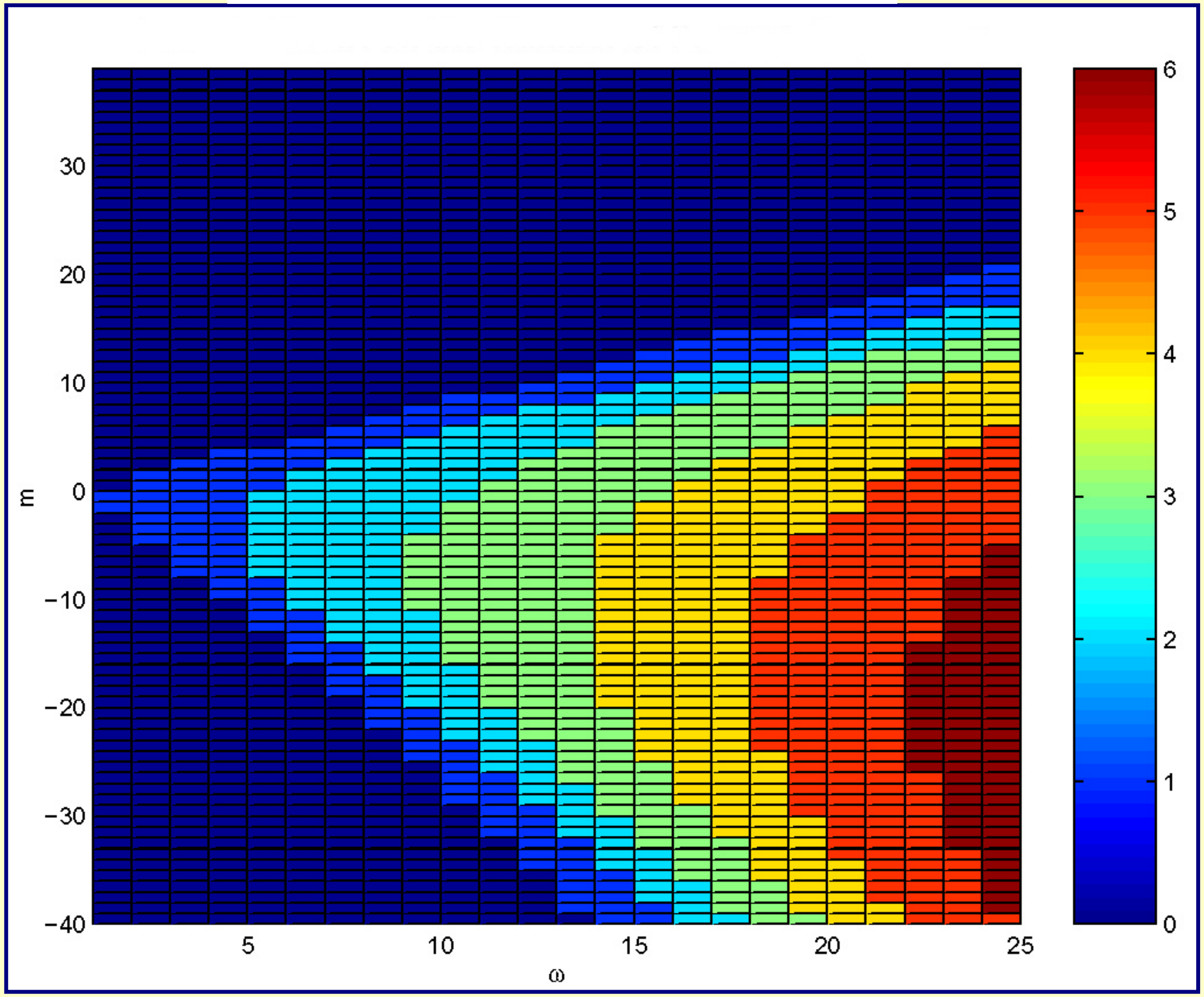

Summary of Normal Mode Analysis

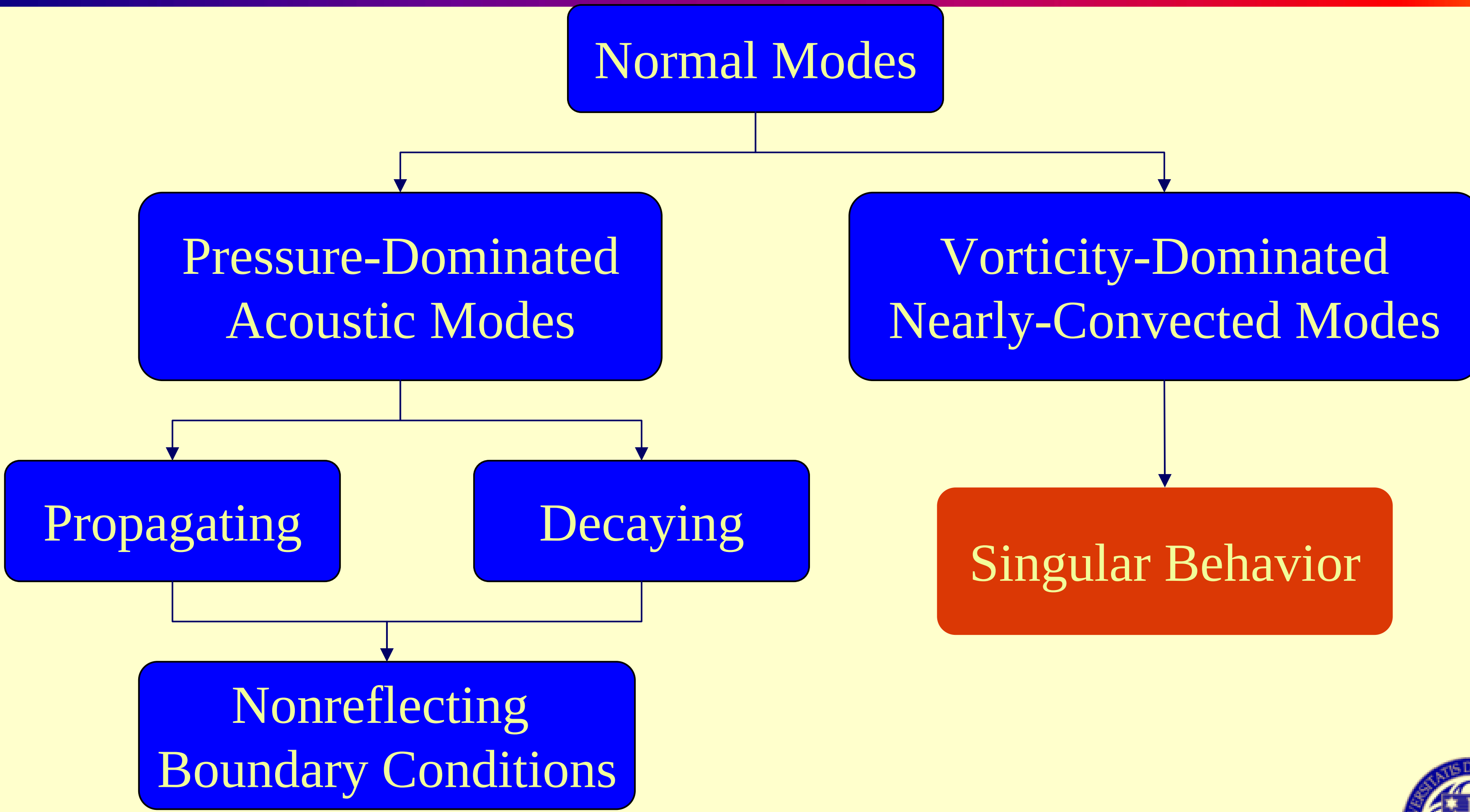

Nonreflecting Boundary Conditions

- Accurate nonreflecting boundary conditions are necessary for computational aeroacoustics

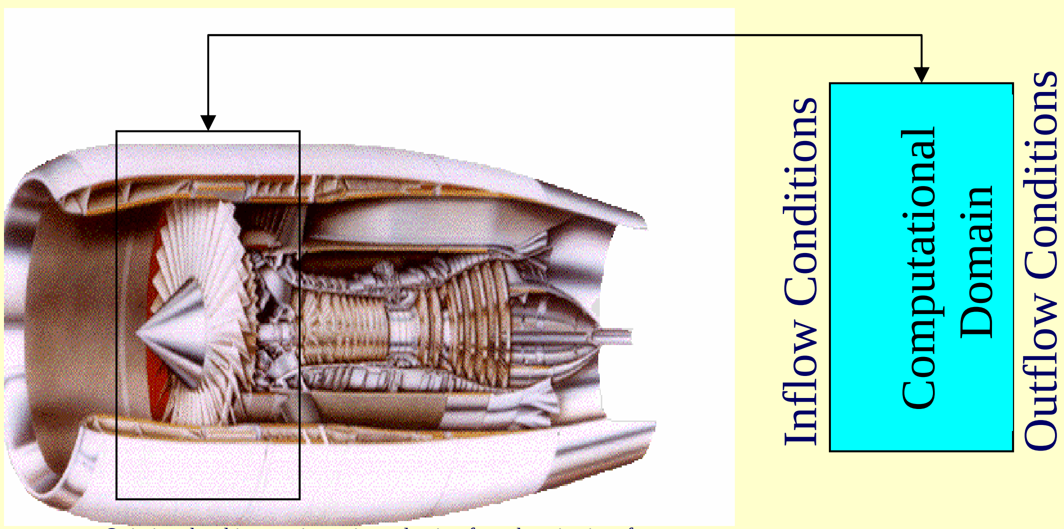

Quieting the skies: engine noise reduction for subsonic aircraft
Advanced subsonic technology program. NASA Lewis research center, Cleveland, Ohio

Formulation

- Presssure at the boundaries is expanded in terms of the acoustic eigenmodes.

$$\boxed{p(\vec{x},t) = \int_{\omega} \sum_{\nu=-\infty}^{\infty} \sum_{n=0}^{\infty} c_{mn}\, p_{mn}(\omega, r)\, e^{i(-\omega\ t + m_{\nu}\theta + k_{mn} x)}\, d\omega}$$

- Only outgoing modes are used in the expansion.
- Group velocity is used to determine outgoing modes.

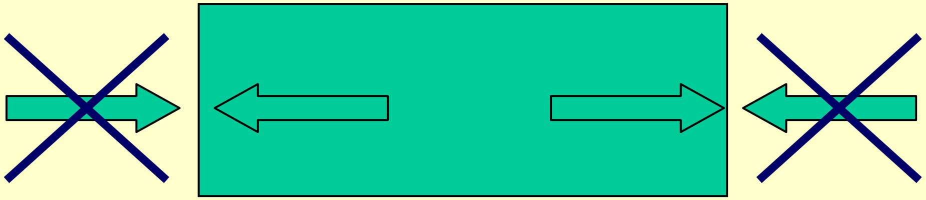

Causality

Nonreflecting Boundary Conditions (Cont.)

$$p(\vec{x},t) = \sum_{\nu=-M/2}^{M/2} \sum_{n=0}^{N} c_{mn}\, p_{mn}(r) e^{i(-\omega t + m_\nu \theta + k_{mn} x)} \quad \Rightarrow \quad [p] = [\Re][c]$$

$$[p]_{L-1} = [\Re]_{L-1}[c]$$

$$[p]_{L} = [\Re]_{L}[c]$$

$$[p]_{L} = [\Re]_{L}[\Re]_{L-1}^{-1}[p]_{L-1}$$

Rotor/Stator Interaction

- The rotor/stator system is decoupled
- The upstream disturbance can be written in the form,

$$\vec{u}_I(r,\theta) = \sum_{m'=-\infty}^{\infty} \vec{a}_{m'}(r) e^{i(m'\theta - \omega t)}$$

$$p_I(r,\theta) = \sum_{m'=-\infty}^{\infty} A_{m'}(r) e^{i(m'\theta - \omega t)}$$

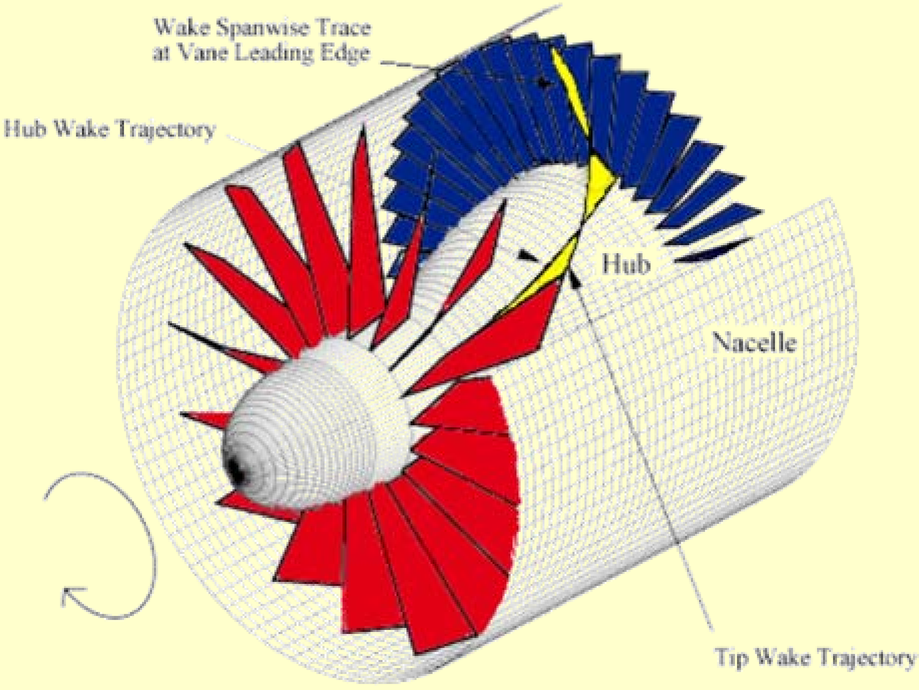

- Quasi-periodic conditions
- Wake discontinuity
- Nonreflecting conditions

Numerical Formulation

- The rotor/stator system is decoupled
- The upstream disturbance can be written in the form,

$$\vec{u}_I(r,\theta) = \sum_{m'=-\infty}^{\infty} \vec{a}_{m'}(r) e^{i(m'\theta - \omega t)}$$

$$p_I(r,\theta) = \sum_{m'=-\infty}^{\infty} A_{m'}(r) e^{i(m'\theta - \omega t)}$$

- Quasi-periodic conditions
- Wake discontinuity
- Nonreflecting conditions

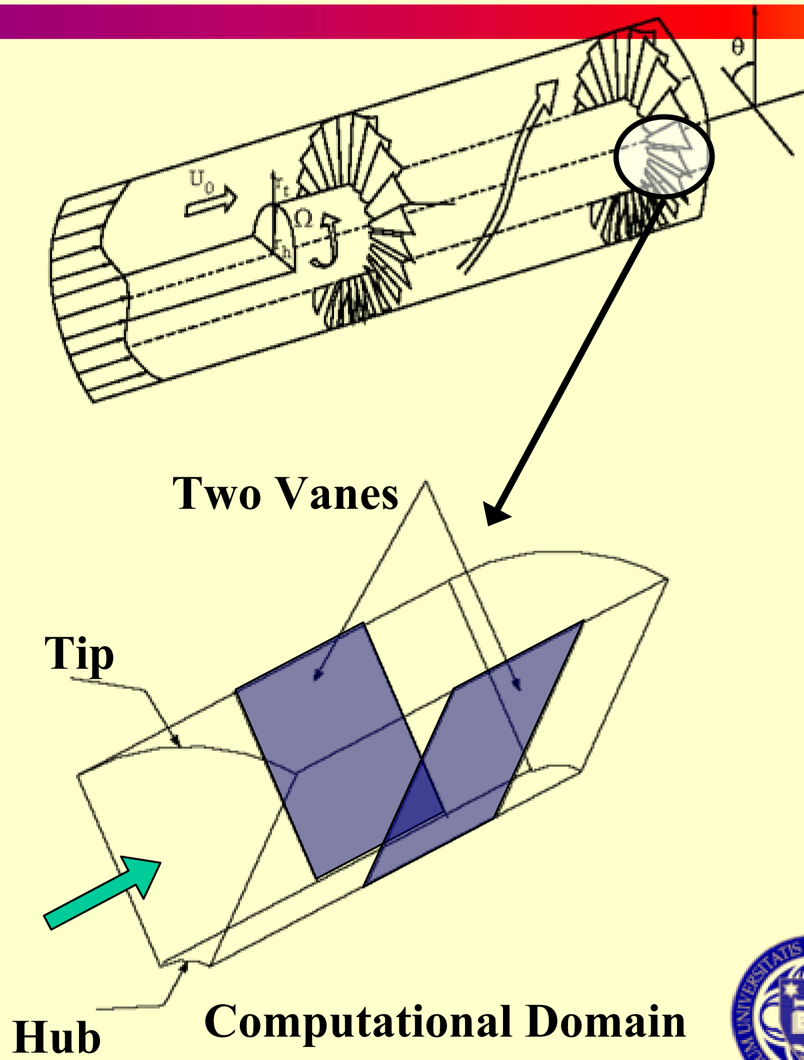

Domain Decomposition
Inner and Outer Regions

Vorticity and Pressure are Coupled.
Solution is Simplified by Removing Phase.

Vorticity and Pressure
Are uncoupled.

O(R)

O(c)

Scattering Results

Parameters for Swirling Flow Test Problem

Narrow Annulus		Full Annulus		Data	
r_{tip}/r_{hub}	1.0/0.98	r_{tip}/r_{hub}	1.0/0.75	M (mach number)	0.5
ω	$0.5\pi, 1.0\pi$ $1.5\pi, 2.0\pi$ $2.5\pi, 3.0\pi$ $3.5\pi, 4.0\pi$	ω	3.0π	α (disturbance)	0.1
				B (rotor blades)	16
				V (stator blades)	24
				C (chord)	$2\pi/V$
				Stagger	45^o
				L (length)	3c

Computational Domain

B (rotor blades)	16
V (stator blades)	24
C (chord)	$2\pi/V$
L (length)	3c

$$\omega = \frac{nB\Omega r_m}{c_o} \approx \mathcal{O}(nB)$$

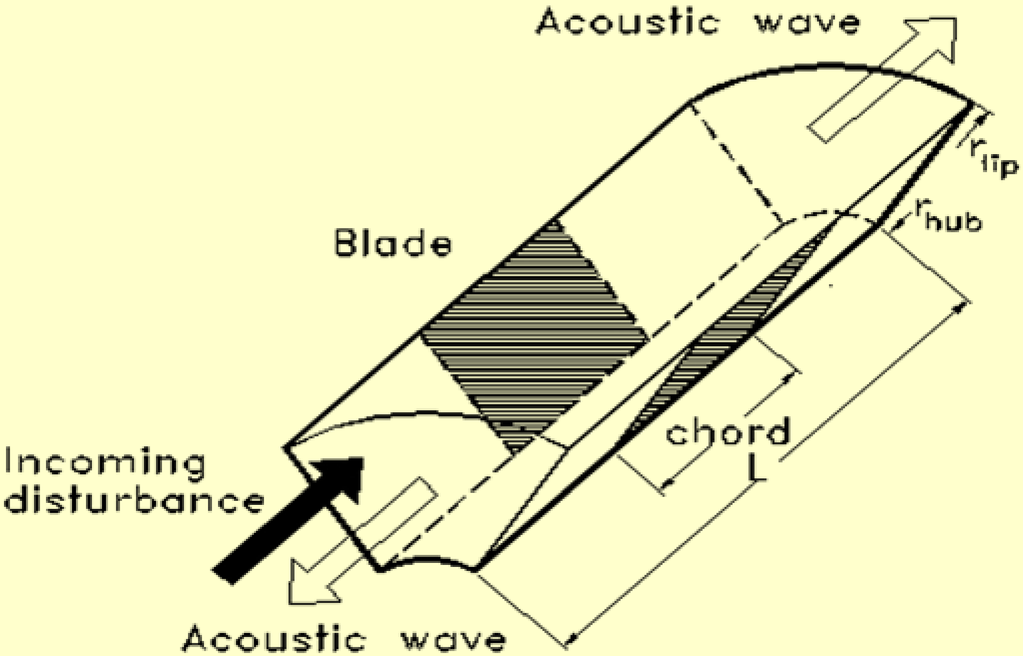

Narrow Annulus Limit

r_{tip}/r_{hub}	1.0/0.98
ω	1.5π, 4.5π, 6.5π
M	0.5
Stagger	45

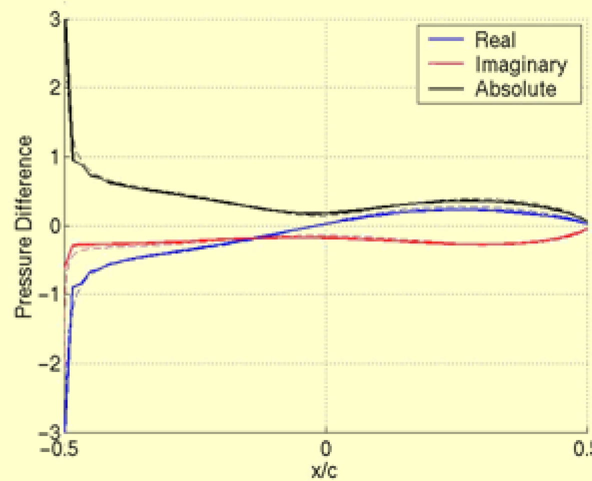

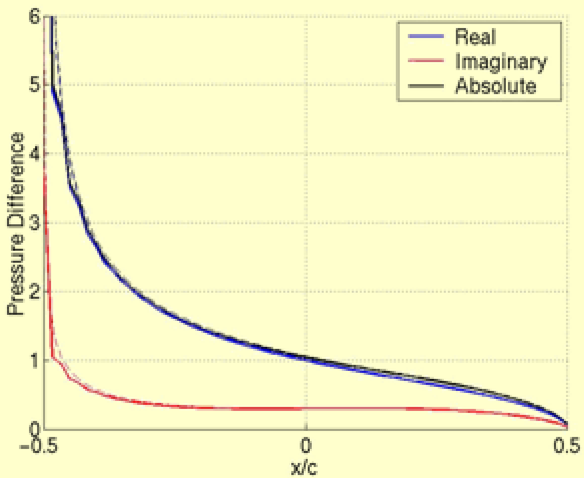

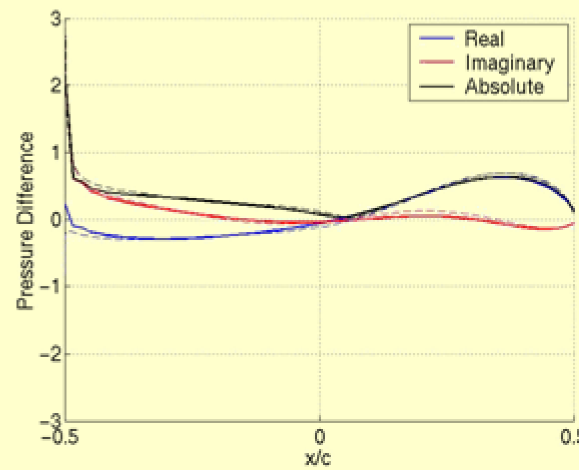

Narrow Annulus Limit

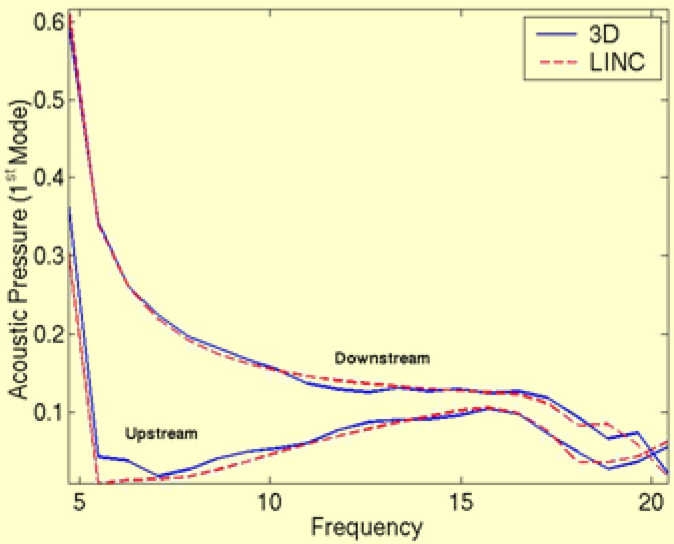

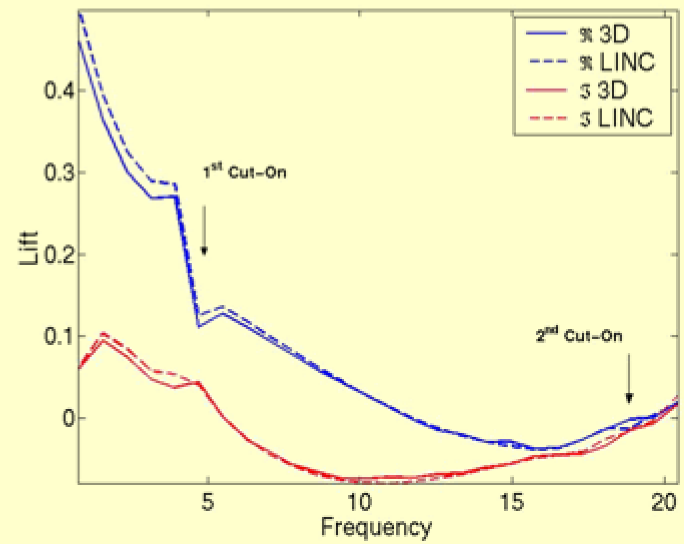

Gust Response for Narrow Annulus Limit –Comparison with 2D cascade

M_o=0.3536, M_θ=0.3536, B=16, V=24, a_r =0

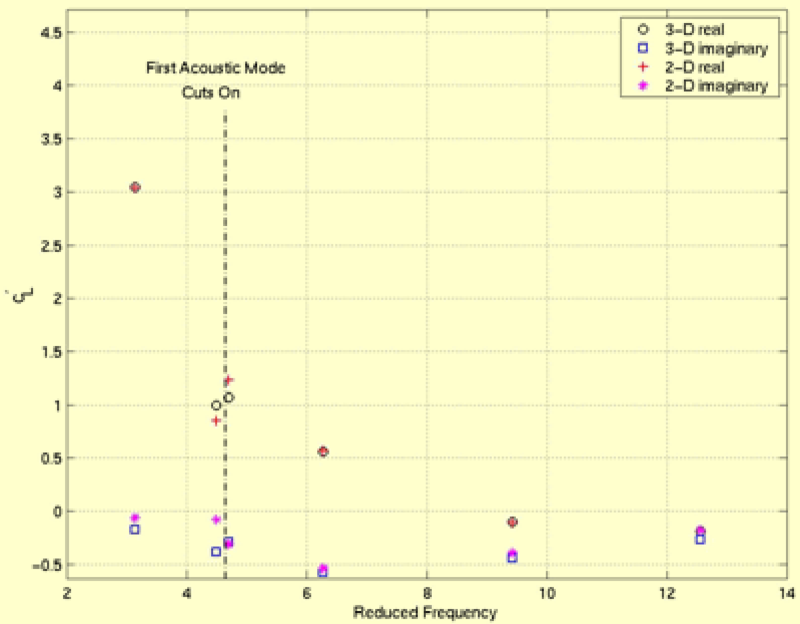

Unsteady Lift Coefficient

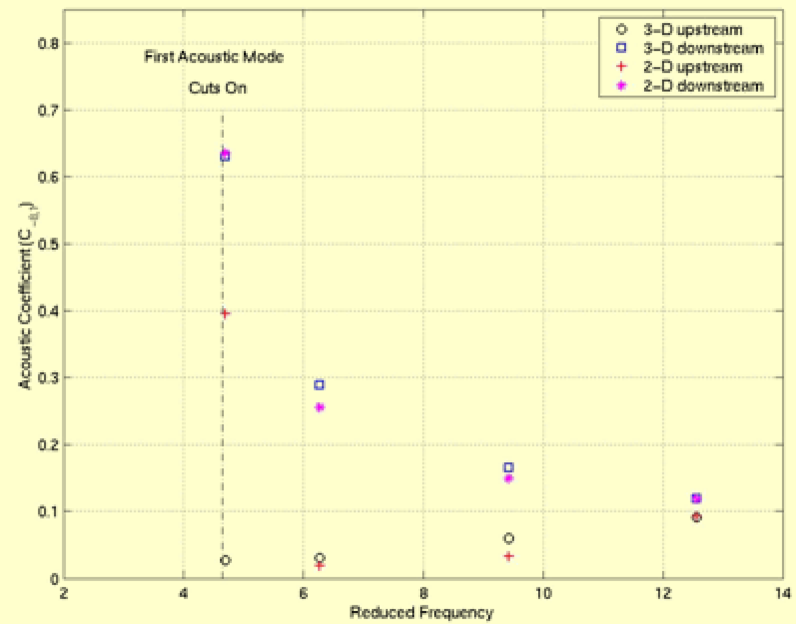

Acoustic Coefficients
m=-8, n=0,1

Gust Response Effect of Hub-Tip Ratio

M_o=0.3536, M_Γ=0.1, M_Ω=0.1, ω=3π, and a_r =0

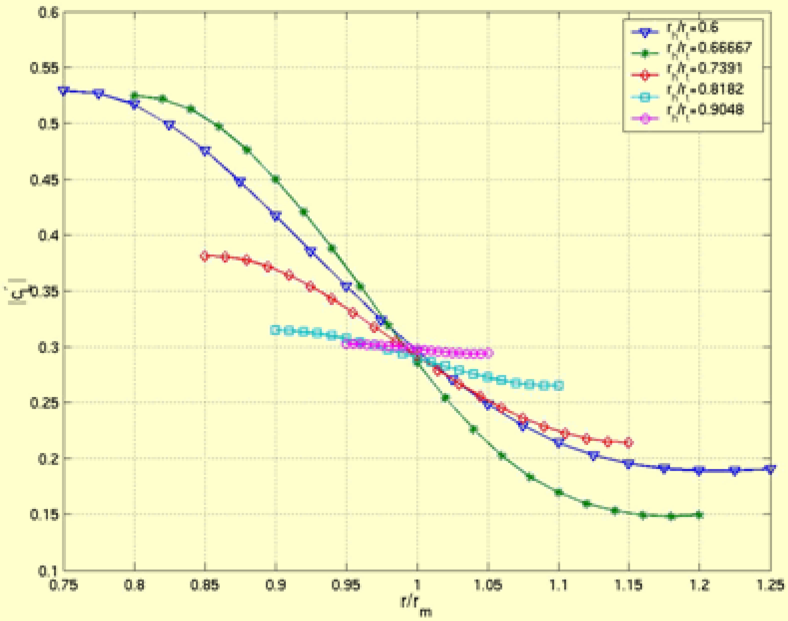

Unsteady Lift Coefficient

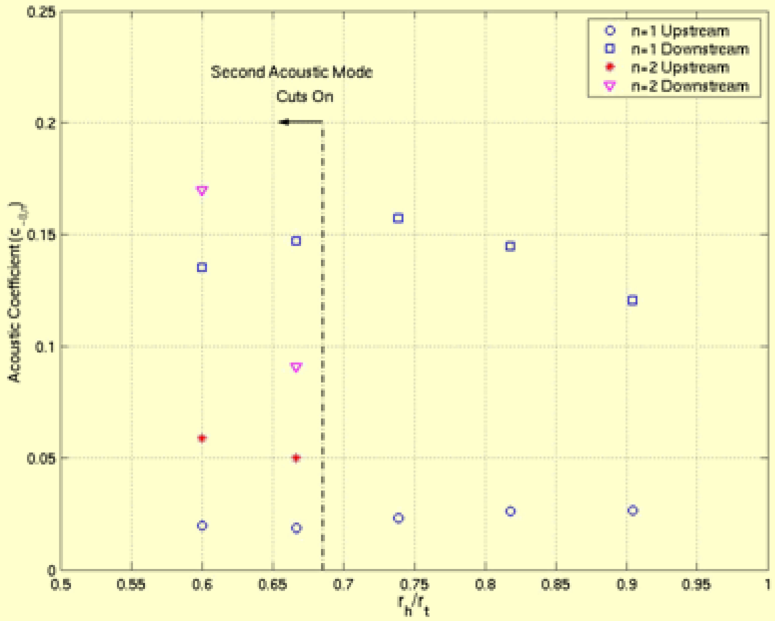

Acoustic Coefficients
m=-8, n=0,1

Mean Flow Cases

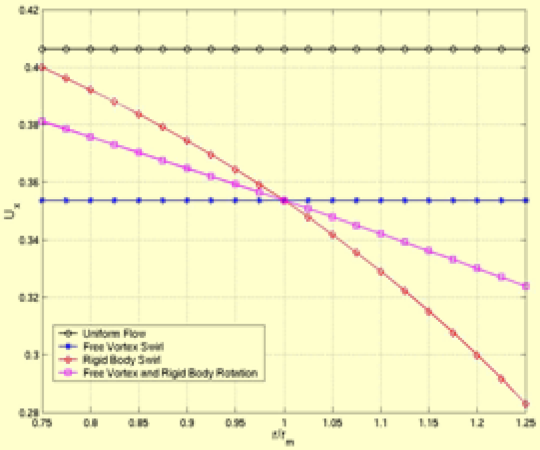

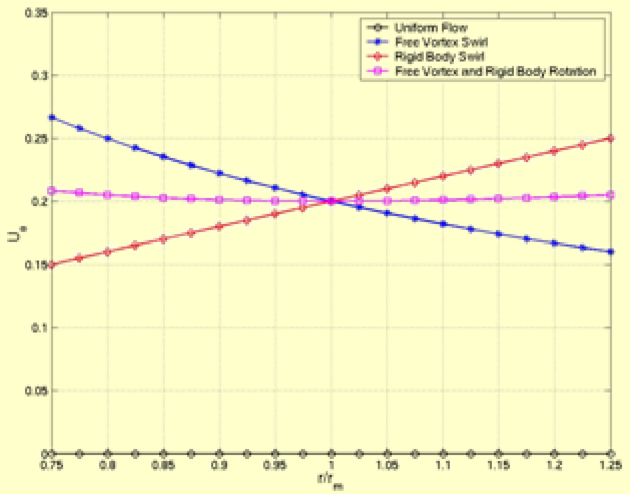

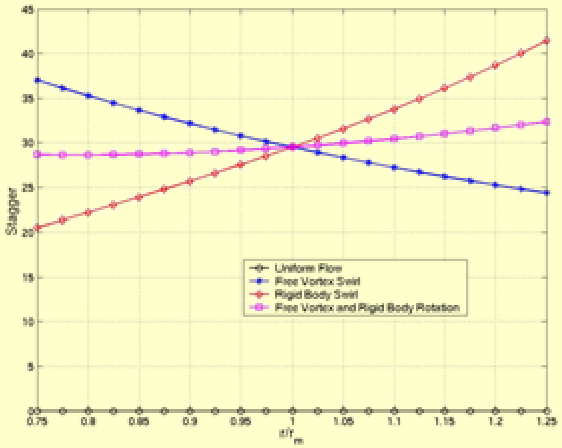

Mean Flow 1: M_o=0.4062, M_Γ=0., M_Ω=0.

Mean Flow 2: M_o=0.3536, M_Γ=0.2, M_Ω=0.

Mean Flow 3: M_o=0.3536, M_Γ=0., M_Ω=0.2

Mean Flow 4: M_o=0.3536, M_Γ=0.1, M_Ω=0.1

Effect of Mean Flow

$r_h \backslash r_t = 0.6$, $\omega = 3\pi$, and $a_r = 0$

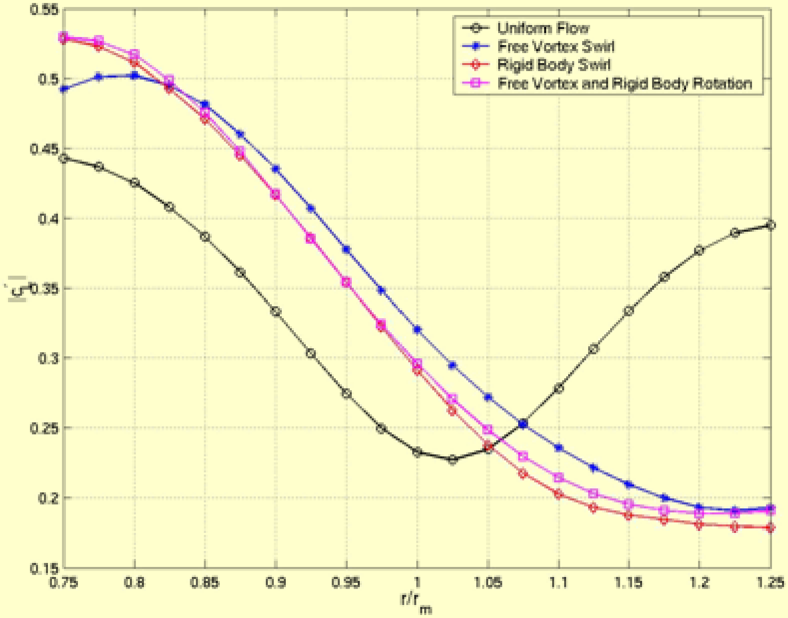

Mode m=-8	Mean Flow 1	Mean Flow 2	Mean Flow 3	Mean flow 4
Downstream n=0	0.2015	0.1610	0.1375	0.1349
Downstream n=1	Cut off	0.0787	0.2140	0.1698
Upstream n=0	0.1363	0.0143	0.0313	0.0195
Upstream n=1	Cut off	0.0370	0.0763	0.0586

Unsteady Lift Coefficient **Acoustic Coefficients**

Effect of Frequency

Mean Flow 4

M_o=0.3536, M_Γ=0.1, M_Ω=0.1, r_h / r_t =0.6667, and a_r =0

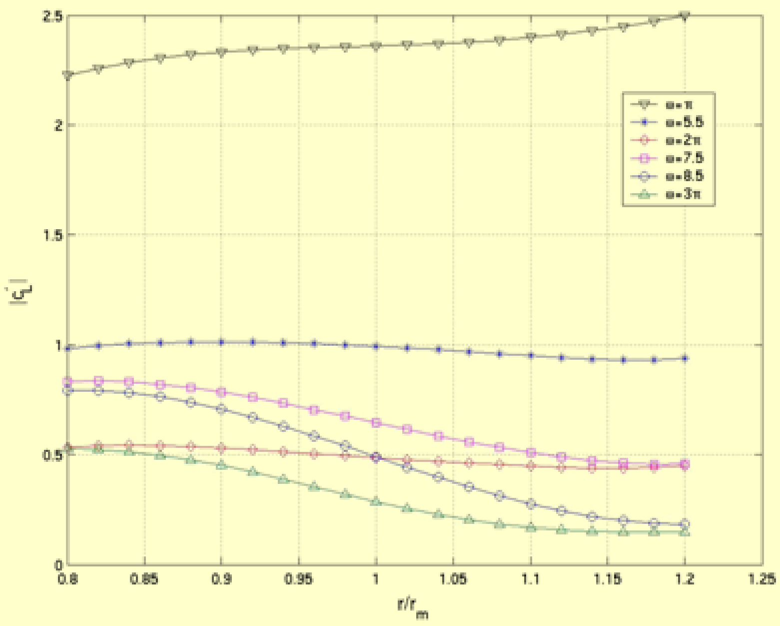

Unsteady Lift Coefficient

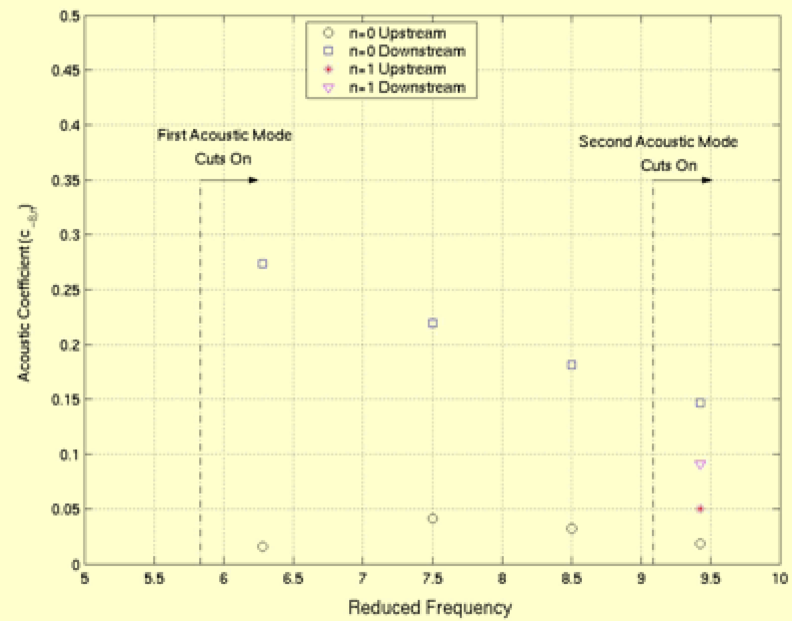

Acoustic Coefficients

m=-8, n=0,1

Effect of the Upstream Disturbance radial component

M_o=0.3536, M_Γ=0.1, M_Ω=0.1, r_h / r_t =0.6667, and $\omega=3\pi$

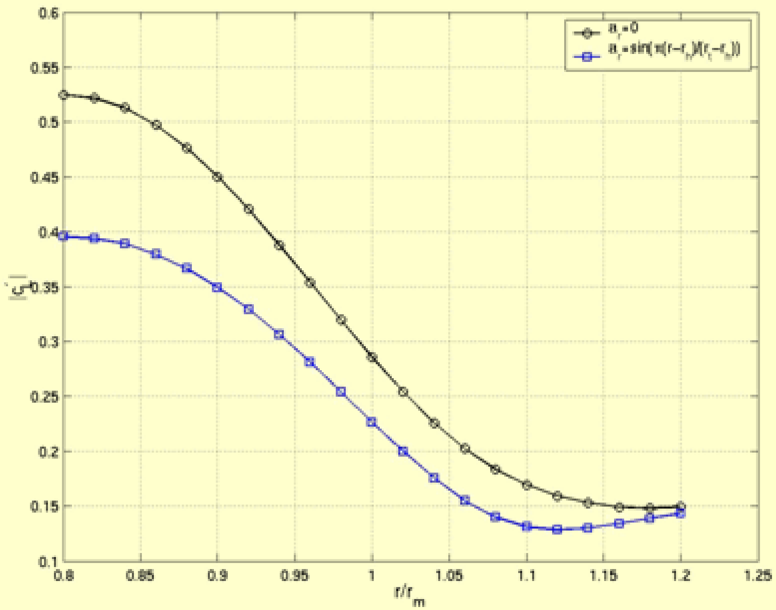

Unsteady Lift Coefficient

Mode m=-8	2-D Disturbance	3-D Disturbance
Downstream n=0	0.1471	0.1094
Downstream n=1	0.0908	0.0617
Upstream n=0	0.0185	0.0143
Upstream n=1	0.0498	0.0418

Acoustic Coefficients

Scattering of Acoustic versus Vortical Disturbance

M_o=0.3536, M_Γ=0.1, M_Ω=0.1, r_h / r_t =0.6667, and ω=3π

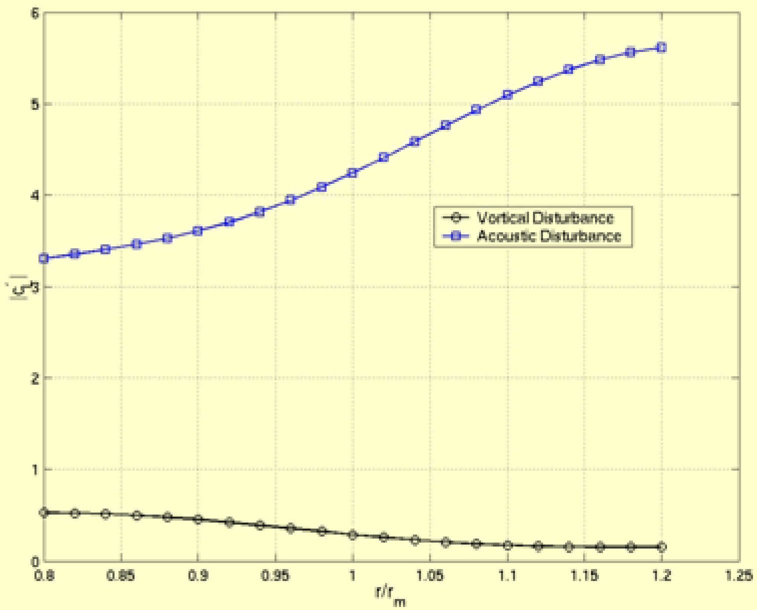

Unsteady Lift Coefficient

Mode m=-8	Vortical Disturbance	Acoustic Disturbance
Downstream n=0	0.1471	0.8608
Downstream n=1	0.0908	0.1458
Upstream n=0	0.0185	0.0718
Upstream n=1	0.0498	0.0775

Acoustic Coefficients

Comparison of Successive Iterations

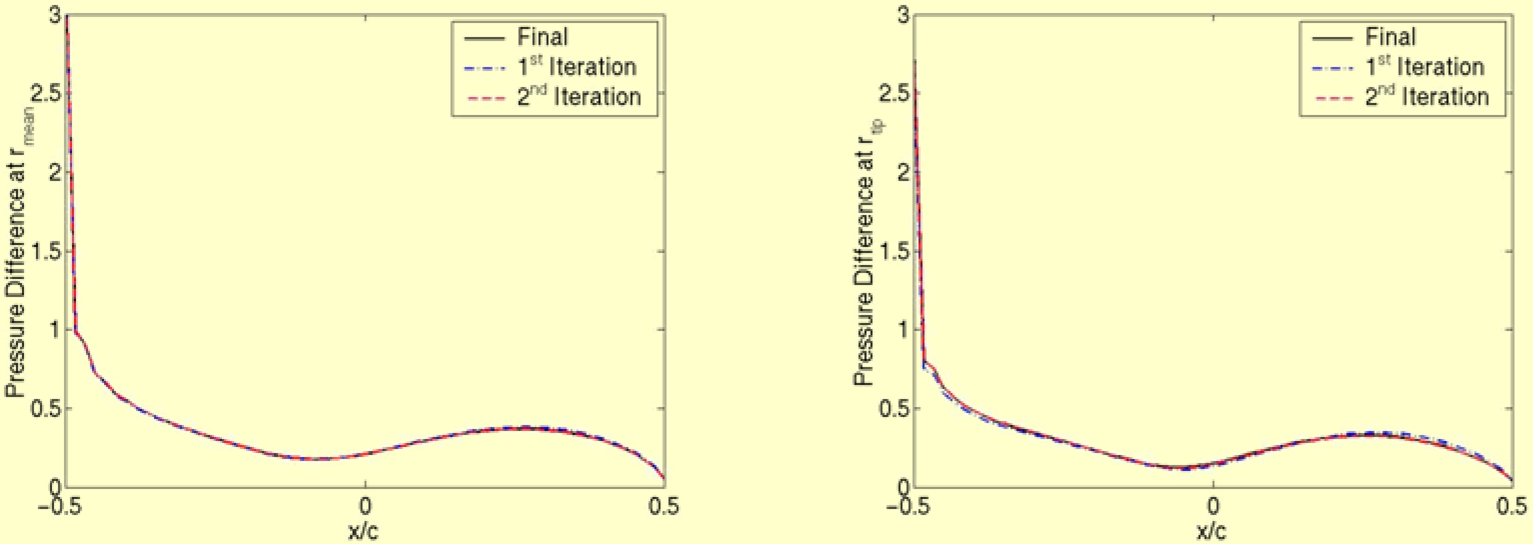

Three-Dimensional Effects Comparison With Strip Theory

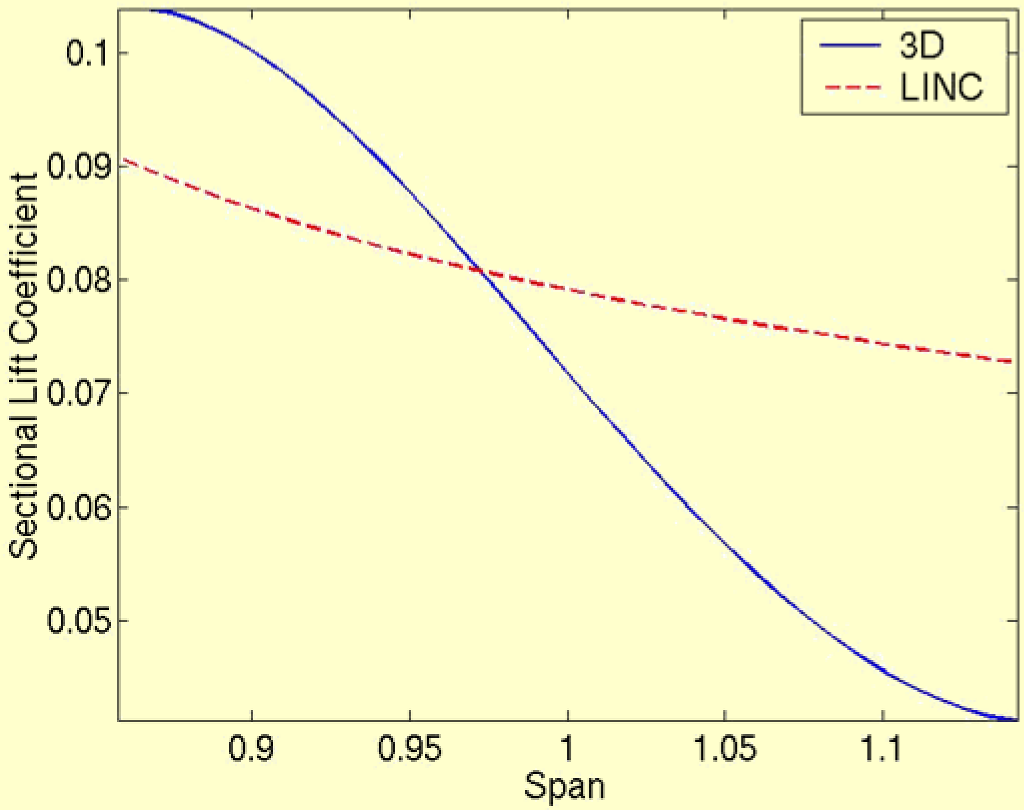

Effect of Swirl

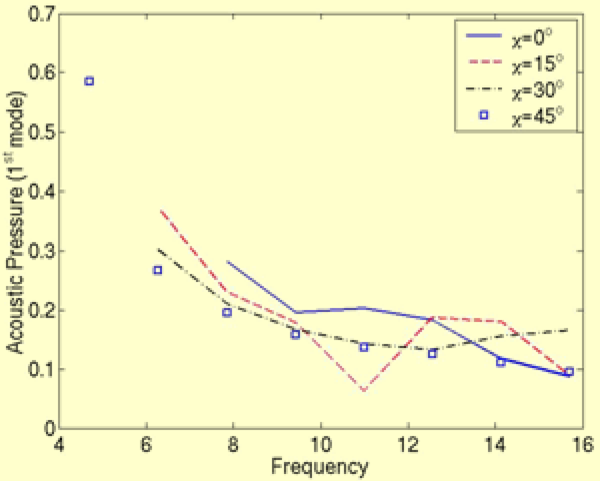

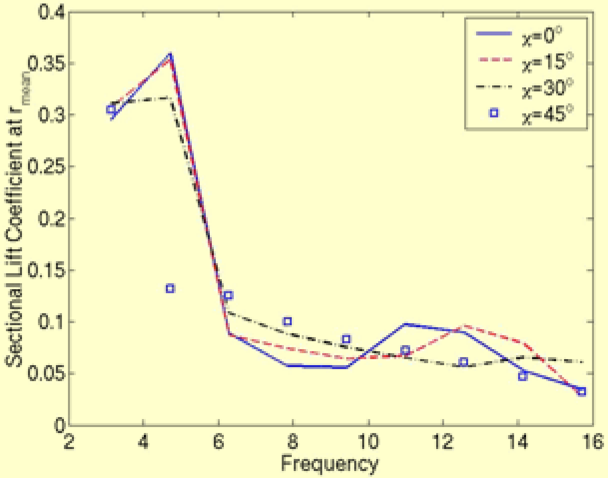

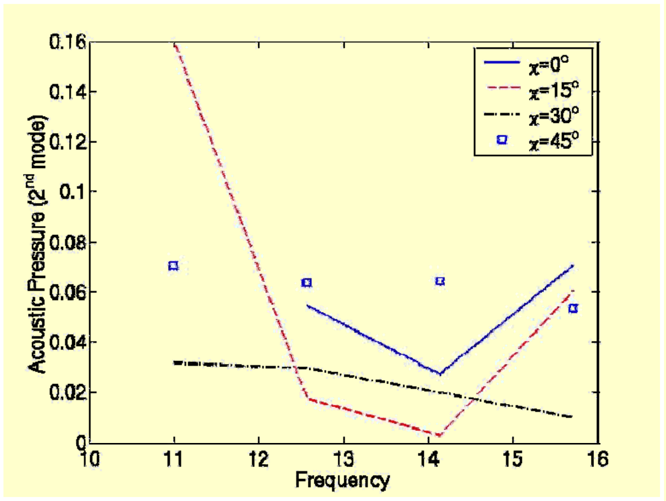

Effect of Blade Twist

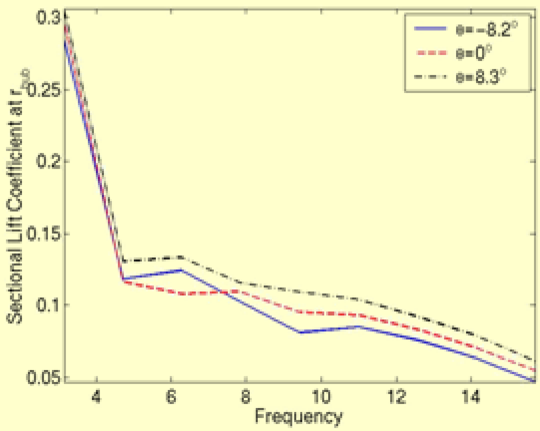

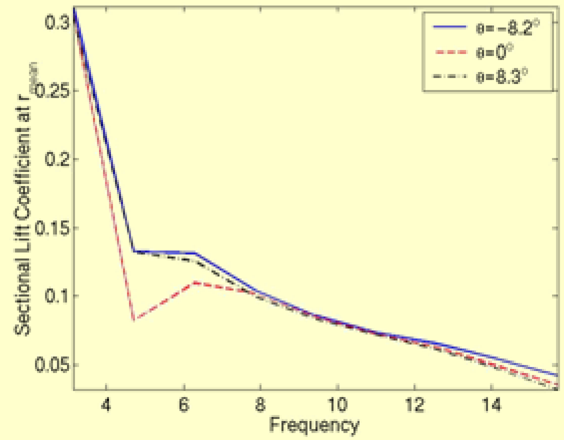

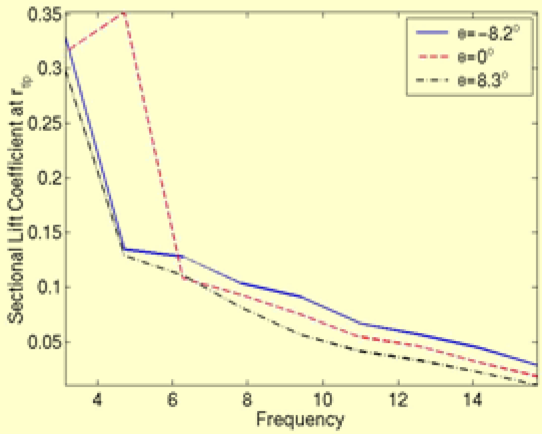

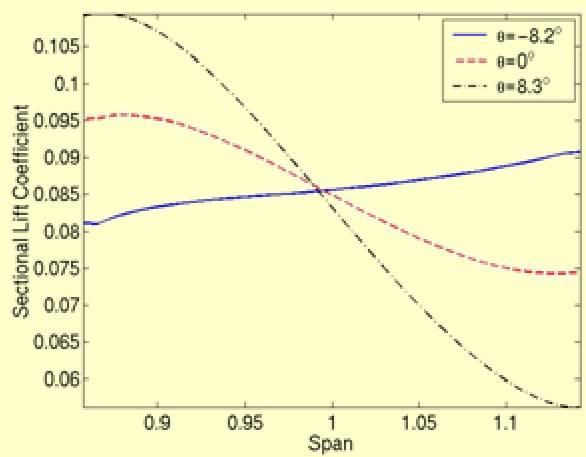

Conclusions

- Swirl affects the impedance of the duct and the number of cut-on acoustic modes. The spinning modes are not symmetric.
- Strip theory gives good approximation as long as there is no acoustic propagation.
- Resonant conditions in strip theory are much more pronounced than for 3D, i.e., lift variation in 3D is much smoother along span.
- Discrepancies between strip theory and 3D calculations increase with the reduced frequency: it is a high frequency phenomenon.